NASA TECHNICAL NOTE

NASA TN D-6385

NASA TN D-6385

ELECTRON AND BREMSSTRAHLUNG PENETRATION AND DOSE CALCULATION

by John W. Watts, Jr., and M. O. Burrell

George C. Marshall Space Flight Center
Marshall Space Flight Center, Ala. 35812

NATIONAL AERONAUTICS AND SPACE ADMINISTRATION • WASHINGTON, D. C. • JUNE 1971

1. Report No.	2. Government Accession No.	3. Recipient's Catalog No.
NASA TN D-6385		

4. Title and Subtitle

Electron and Bremsstrahlung Penetration and Dose Calculation

5. Report Date
June 1971

6. Performing Organization Code

7. Author(s)

John W. Watts, Jr., and M. O. Burrell

8. Performing Organization Report No.
M440

9. Performing Organization Name and Address

George C. Marshall Space Flight Center
Marshall Space Flight Center, Alabama 35812

10. Work Unit No.
124-09-21-8023

11. Contract or Grant No.

12. Sponsoring Agency Name and Address

National Aeronautics and Space Administration
Washington, D. C. 20546

13. Type of Report and Period Covered
Technical Note

14. Sponsoring Agency Code

15. Supplementary Notes

Prepared by Space Sciences Laboratory, Science and Engineering.

16. Abstract

Various techniques for calculation of electron and bremsstrahlung dose deposition are described. New energy deposition, transmission, and reflection coefficients for electrons incident on plane slabs for angles of 0, 30, 60, 75, and 89.9 deg and energies of 0.5, 1.0, 2.0, 3.0, 4.0, 5.0, 6.0, and 10.0 MeV are presented, and methods for their use in electron dose calculations are developed. A method for electron dose calculations using the "straight-ahead" approximation is also developed and the various methods are compared and found to be in good agreement. Accurate and approximate methods of calculating bremsstrahlung dose are also derived and compared.

17. Key Words (Suggested by Author(s))	18. Distribution Statement
Electron transport Bremsstrahlung transport Dose calculations	Unclassified Unlimited

19. Security Classif. (of this report)	20. Security Classif. (of this page)	21. No. of Pages	22. Price*
Unclassified	Unclassified	96	$3.00

*For sale by the National Technical Information Service, Springfield, Virginia 22151

TABLE OF CONTENTS

TABLE OF CONTENTS (Concluded)

LIST OF ILLUSTRATIONS

LIST OF ILLUSTRATIONS (Concluded)

LIST OF TABLES

LIST OF TABLES (Continued)

LIST OF TABLES (Concluded)

ACKNOWLEDGMENT

We would like to acknowledge the help of Jame E. Derrickson who set up and ran the Berger computer program ETRAN and of Lou Hall who did much of the curve fitting and the data reduction.

ELECTRON AND BREMSSTRAHLUNG PENETRATION AND DOSE CALCULATION

SUMMARY

Sources of high-energy electrons are encountered in space (the magnetically trapped Van Allen belt electrons) and in ground-level high-energy physics laboratories. It is important to be able to predict the damage resulting to human beings and radiation-sensitive equipment near these sources. In this report, various techniques for the calculation of electron and bremsstrahlung dose deposition are described. New energy deposition, transmission, and reflection coefficients for electrons incident on plane slabs for angles of 0, 30, 60, 75, and 89.9 deg and energies of 0.5, 1.0, 2.0, 3.0, 4.0, 5.0, 6.0, and 10.0 MeV are presented, and methods for their use in electron dose calculations are developed. A method for electron dose calculations using the "straight-ahead" approximation is also developed, and the various methods are compared and found to be in good agreement. Accurate and approximate methods of calculating bremsstrahlung dose are derived and compared. The approximation is found to give good order of magnitude estimate of dose where the electron spectrum falls off exponentially with energy. The primary weakness of both calculations is the approximation of the bremsstrahlung source angular distribution; the actual distribution is not easily determined. More work needs to be done in this area.

INTRODUCTION

As man has moved out into space, one of the problems confronting him has been damage caused by the various types of radiation encountered. Inside the geomagnetosphere one of the major components of the radiation environment consists of high-energy, magnetically trapped electrons. Fluxes higher than 1.58×10^8 e/cm^2-sec with energies above 0.5 MeV [1] have been observed near the middle of the Van Allen belts. Fluxes this high can cause very significant problems for men and radiation-sensitive equipment behind thin shields (less than 4g/cm^2 thick) where the primary electrons are still present and thicker shields which electrons induced bremsstrahlung penetrate.

The determination of the damage due to electrons at a given point in a spacecraft is a three-part problem. First, the energy and angular flux

1. To convert electron volts to SI Units in joules, multiply by 1.60210×10^{-19}.

distribution of electrons incident over the surface of the vehicle must be found; second, this exterior distribution must be transformed into the distribution at the point of interest; and finally, interior distribution is used to determine a secondary source distribution or some damage criteria such as dose, number deposition, charge deposition, etc. Obviously, each problem of this type must be treated individually because of the complexity of the geometry and the exterior particle distribution involved. Since the primary interest here is in the second part of the problem, for ease of comparison with other results and to emphasize parameters of primary importance, consideration will be confined to a fairly simple model problem. However, the methods described can be applied to more complex situations. The geometry consists of an infinite plane slab in front of a point receiver (Fig. 1). The incident energy spectrum is arbitrary but limited to energies below about 10.0 MeV. The two extreme cases of angular distributions, isotropic (cosine currents) and monodirectional incidence, will be examined.

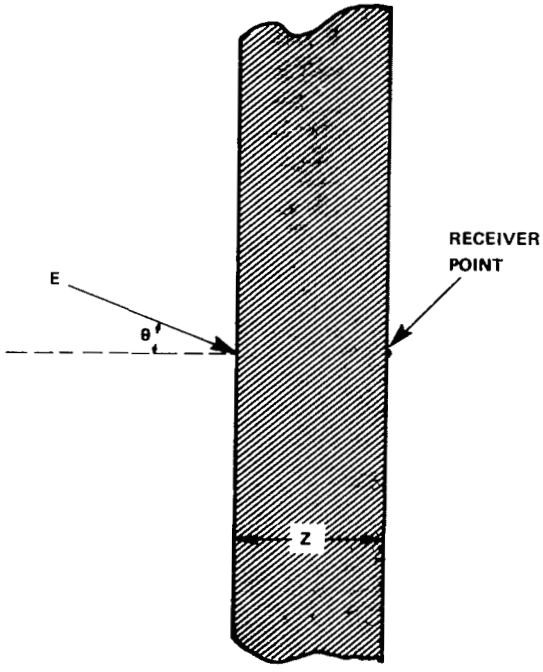

Figure 1. Basic Geometry used for calculations.

ELECTRON INTERACTION WITH MATTER

To solve any particle transport problem one must first understand the basic interactions possible and have some estimate of each one's importance as an energy loss and scattering mechanism and as a secondary particle production source. In the energy range of interest (0.1 — 10.0 MeV) there are two important types of interactions for electrons, both of them electromagnetic. Scattering from atomic electrons can result in loss of up to half of the energy of an electron with a resulting large change in direction, although the average electron-electron scatter does not result in such large changes. Secondaries produced in the interactions include secondary electrons from ionized atoms, auger electrons and x-rays due to de-excitation of excited atoms, and some electron-electron bremsstrahlung. With the exception of secondary electrons from ionized atoms these secondaries are not

particularly important because of their low energies or numbers. Though low in energy the secondary electrons are important in any number deposition calculation.

The other important interaction is coulombic scattering from the nuclei of atoms. This is a primary energy loss and scattering mechanism because so many interactions of this type occur per unit pathlength. For example, Berger [2] estimates that in the course of slowing down from 0.5 to 0.25 MeV in aluminum an electron undergoes 2.9×10^4 collisions assuming a Rutherford scattering cross section with a screening correction. Thus the average loss per scatter is less than 10 eV. Because the mass of a nucleus is high relative to that of an electron, little energy is lost through motion of the nucleus. Large energy losses do occur from bremsstrahlung produced as the electron accelerates and decelerates in passing through the nuclear electric field. At low energies (< 1.0 MeV) the energy lost as bremsstrahlung is small compared to that lost by other scattering processes, but the photons produced are important, especially in dose calculations since the more energetic ones penetrate much deeper than the electrons that produce them. At higher energies bremsstrahlung makes an even more significant contribution to the total dose and radiative energy losses are large enough to become important in describing the transport of electrons. At 10.0 MeV 7.721 percent of the initial energy is lost as bremsstrahlung in stopping in aluminum [3].

A completely realistic description of electron transport must be capable of carrying both primary and secondary electrons through many thousands of interactions and setting up a bremsstrahlung source distribution for calculations using one of the many gamma ray transport techniques. Most methods developed for the transport of gamma rays or neutrons have the basic assumption that the incident particle undergoes a relatively small number of interactions of importance in passing through the shield. Thus they are not immediately applicable to electron transport. The intermediate step is the multiple scattering and straggling theory, which can define the angular, energy, and spatial distribution resulting from a number of successive interactions rather than a single interaction. Thus the transport can be divided into larger steps than needed if a single scattering theory were used. A good description of the application of multiple scattering theory to electron Monte Carlo calculations is given by Berger [2].

Probably the most successful attack on the electron transport problem has been by Martin Berger [2-4] using Monte Carlo methods and multiple scattering techniques. His present set of programs will take an incident beam of electrons or photons and follow both the primaries and any secondary electrons or photons produced. The output includes almost any quantity of interest

depending on the program option used. Because the simulation is so thorough, the program is very complex and requires large amounts of computer time on one of the larger machines available to complete an accurate calculation. Thus, the program's primary usefulness is in generating basic data for incorporation into other programs using more simplified approaches to the problem.

Berger's program was made available to Marshall Space Flight Center (MSFC) and a number of calculations have been performed here for comparison with experimental work [5]. As a second study systematic calculations covering the energy range of from 0.5 to 10.0 MeV for a number of angles of incidence by a monodirectional beam on a plane aluminum slab were made. (The geometry is the same as shown in Figure 1.) Of particular interest were the electron energy and number transmission and reflection and the energy deposition coefficients (tabulated in Appendixes A through C), because they can be incorporated into an electron dose or number deposition calculation involving an arbitrary incident electron energy and angular distribution. To minimize the computer time used no photons were followed, and only enough electron histories (2500 through 7000, depending on the angle of incidence) were sampled to get good statistics for the reflection, transmission, and deposition coefficients. (A much higher number of histories would have been required to get good statistics on one of the differential quantities such as exiting energy spectrum.) The fact that secondary photons were not followed means that there is a slight underestimate both in the number of coefficients due to missing tertiary electrons produced by the photons and in the energy factors due to energy transported by secondary photons. Because over most of the energy range of interest electrons lose only a small fraction of their energy as photons, both these effects should be small. The radiative yield, the fraction of an electron's energy lost as bremsstrahlung in stopping, is 0.003324 at 0.25 MeV and 0.07721 at 10.0 MeV in aluminum [3]. This quantity should set an upper bound on the possible error induced by the limitations imposed at least for the energy factors.

USE OF BERGER'S MONTE CARLO DATA IN ELECTRON DOSE CALCULATIONS

There are several approaches for attacking a dose deposition calculation using the results tabulated by Berger's electron transport program. The most obvious is to use the internal energy spectrum and instantaneous stopping power. Two less obvious but more efficient methods — one reasonably exact and the other approximate — will be described here.

The exact calculation makes use of a quantity Berger calls energy deposition, which is the average energy deposited per unit mass per electron at a given depth into a plane, infinitely thick slab by, in this case, a monodirectional beam of electrons. [This does not follow the initial model (Fig. 1) because there is material behind the receiver point.] Berger calculates the energy deposition by breaking up the slab into thin layers and keeping an inventory of energy deposited in each layer and then dividing this quantity by the incident number of initial electron histories and layer thickness. Thus,

$$\rho(E, \theta, X_j) = \frac{\sum_{i=1}^{N_j} \Delta E_{ij}}{N_0 \Delta X_j} \quad , \tag{1}$$

where ρ is the energy deposition in MeV/g/unit current, E is the incident energy in MeV, θ is the incident beam angle measured from the normal to the slab, X_j is the depth to the center of the jth layer, N_j is the number of electrons penetrating layer j, ΔE_{ij} is the energy in MeV deposited by the ith penetrating electron in the jth layer, N_0 is the number of initial electron histories, and ΔX_j is the thickness of the jth layer in g/cm^2. In Berger's tabulation X_j is measured in fractions of an electron pathlength at the incident energy. The electron mean pathlength (tabulated in Appendix D) is the average length of the zig-zag path followed by an electron in stopping as opposed to the mean range which is the average straight-line distance traversed. It is given by

$$r_0(E) = \int_E^0 \frac{dE'}{S_T(E')} \quad , \tag{2}$$

where $r_0(E)$ is the pathlength at energy E and $S_t(E')$ is the total instantaneous stopping power.

If there is an angular and energy flux distribution given by $\Phi_0[E, \vec{\Omega}(\theta, \phi)]$ with Φ_0 electrons incident per unit energy at E and per unit solid angle in the direction $\vec{\Omega}$, then the incident current as used by Berger is

$$J_0(\vec{\Omega}) = \Phi_0(E, \vec{\Omega}) \cos(\theta) \quad , \tag{3}$$

and the dose at a depth Z in g/cm^2 is by

$$D(Z) = K \int_{\vec{\Omega}} \int_{E} \rho\,[E, \theta, Z/r_0(E)]\, \Phi_0\,(E, \vec{\Omega}) \cos\theta\, dE\, d\vec{\Omega} \quad , \tag{4}$$

where K is a units conversion constant. Dose is more often measured in rads than MeV/g, in which case $K = 1.60 \times 10^{-8}$ rads/(MeV/g).[2] In the case where there is a monodirectional beam incident at an angle θ from the slab normal, equation (4) becomes

$$D(Z, \theta) = K \cos\theta \int_{E} \rho[E, \theta, Z/r_0(E)]\, \Phi_0\,(E)\, dE \quad . \tag{5}$$

Another case of interest is that in which the distribution is half-space isotropic. In this case the dose is given as

$$D_{iso}(Z) = K \int_{E} \int_{0}^{\frac{\pi}{2}} \rho[E, \theta, Z/r_0(E)] \cos\theta \sin\theta\, d\theta\, \Phi_0\,(E)\, dE \quad . \tag{6}$$

Thus, a half-space energy deposition function may be defined by

$$\rho_{iso}\,(E, X) = \int_{0}^{\frac{\pi}{2}} \rho(E, \theta, X) \cos\theta \sin\theta\, d\theta \quad . \tag{7}$$

This function is tabulated in Appendix E. If equation (7) is used, equation (6) becomes

$$D_{iso}(Z) = K \int_{E} \rho_{iso}\,[E,\ Z/r_0(E)]\, \Phi_0\,(E)\, dE \quad . \tag{8}$$

2. To convert rads to SI Units in joules per kilogram, multiply rads by 0.01.

The approximate method for calculating electron dose makes use of the energy transmission and reflection factor of Berger to derive an approximation to the energy deposition function. The electron energy current transmission and reflection and number current transmission and reflection factor tabulated in Appendixes A and B are defined as follows:

$$
\begin{aligned}
T_N(E,\theta,X) &= \frac{N_T(E,\theta,X)}{J_0(\theta)} \\
A_N(E,\theta,X) &= \frac{N_R(E,\theta,X)}{J_0(\theta)} \\
T_E(E,\theta,X) &= \frac{\sum_{i=1}^{N_T} E_{Ti}(E,\theta,X)}{E\,J_0(\theta)} \\
A_E(E,\theta,X) &= \frac{\sum_{i=1}^{N_R} E_{Ri}(E,\theta,X)}{E\,J_0(\theta)} \quad ,
\end{aligned}
\tag{9}
$$

where T_N is the number transmission factor; N_T is the number of electrons passing through a slab X thick; A_N is the number reflection factor where N_R is the number of electrons reflected from a slab X thick; T_E is the energy transmission factor where E_{Ti} is the energy of the ith transmitted electron; A_E is the energy reflection factor where E_{Ri} is the energy of the ith reflected electron; and $J_0(\theta)$ is the incident current.

How these factors may be used in energy deposition or dose calculations will now be considered. From conservation of energy,

$$
E = E\,[A_E(E,\theta,X) + U_E(E,\theta,X) + T_E(E,\theta,X)] \tag{10}
$$

or

$$
1 = A_E(E,\theta,X) + U_E(E,\theta,X) + T_E(E,\theta,X) \tag{11}
$$

is obtained, where $U_E(E,\theta,X)$ is the fraction of the energy either deposited in the slab or radiated as bremsstrahlung. Since in the energy range of interest the radiated component is small, it will be assumed negligible. If a quantity $f(X',E,\theta,X)\,dX'$ is defined, which is the fraction of the incident energy deposited between X' and $X' + dX'$, then

$$U_E(E,\theta,X) = \int_0^X f(X',E,\theta,X)\,dX' \quad . \tag{12}$$

Using equations (11) and (12) yields

$$\int_0^X f(X',E,\theta,X)\,dX' = 1 - A_E(E,\theta,X) - T_E(E,\theta,X) \quad . \tag{13}$$

Taking the derivative with respect to X gives

$$f(X,E,\theta,X) + \int_0^X \frac{df}{dX}(X',E,\theta,X)\,dX' = -\frac{d}{dX}\left[A_E(E,\theta,X) + T_E(E,\theta,X\right] \quad . \tag{14}$$

The approximation in this method involves ignoring the integral term on the left in this equation. Since $f(X',E,\theta,X)$ increases with increasing X (due to reflected electrons) the derivative is always greater than or equal to zero. Thus the integral is positive, and ignoring it gives a conservative estimate of $f(X,E,\theta,X)$. It is difficult to justify this approximation except to observe that in practice it yields results comparable with those of the previously described method. It was developed because Berger's older publication presented only the transmission and reflection factors, the energy deposition factor having become available only recently.

The energy deposition function (in units of MeV/g) is given by

$$\rho(X,E,\theta,X) = \frac{Ef(X,E,\theta,X)}{r_0(E)} \tag{15}$$

or

$$\rho(X,E,\theta,X) \approx \frac{-E}{r_0(E)}\frac{d}{dX}\left[A_E(E,\theta,X) + T_E(E,\theta,X)\right] \quad . \tag{16}$$

It is interesting to note that $f(X', E, \theta, X)$ for $X' < X$ always has a contribution caused by reflection from portions of the shield beyond X' but that $f(X, E, \theta, X)$ does not. Thus it approximates the quantity needed for an energy deposition calculation in our original geometry.

Because of the definition of ρ in the derivations the material of the receiver must be the same as that of the shield. An approximate correction for estimating the dose for a different receiver can be made by multiplying the single material calculation by the ratio of the collision stopping power in the receiver material to the collision stopping power in the shield material at some typical energy for the exiting electron spectrum. Fortunately, the energy selected is not particularly important since the ratio of two electron stopping powers is not a sensitive function of energy except at very low energies (> 0.01 MeV). Some estimate of the accuracy of the approximation can be found by observing the variation of the ratio with energy. A particularly interesting case is that of an aluminum shield and a tissue receiver. This case, using Berger's stopping power data [3], is given in Table 1.

TABLE 1. RATIO OF TISSUE COLLISION STOPPING POWER TO ALUMINUM COLLISION STOPPING POWER AS A FUNCTION OF ENERGY

Energy (MeV)	$R = \frac{\frac{dE}{dX}\text{tissue}}{\frac{dE}{dX}\text{aluminum}}$	$\frac{R-1.3}{R} \times 100$ (%)
0.01	1.383	6.0
0.02	1.350	3.7
0.04	1.325	1.9
0.06	1.313	1.0
0.08	1.305	0.4
0.1	1.300	0.0
0.2	1.285	-1.2
0.4	1.276	-1.9
0.6	1.272	-2.2
0.8	1.271	-2.3
1.0	1.272	-2.2
2.0	1.281	-1.5
4.0	1.301	0.1
6.0	1.317	1.3
8.0	1.329	2.2
10.0	1.340	3.0

Taking the simple average of ratios between energies of 0.1 to 10.0 MeV yields a correction (1.30) that will be within about 3 percent of an exact calculation under most conceivable conditions. (For typical incident energy spectra encountered it would be unusual for the average energy of the exiting spectrum to be less than 0.04 MeV). Thus, for an aluminum shield and a tissue receiver equations (5) and (6) become, respectively,

$$D(Z,\theta) = 1.3\,K\cos\theta \int_E \rho\,[E,\theta,Z/r_0(E)]\;\Phi_0(E)\;dE \qquad (17)$$

and

$$D_{iso}(Z) = 1.3\,K \int_E \rho_{iso}\,[E,Z/r_0(E)]\;\Phi_0(E)\;dE \quad . \qquad (18)$$

Curve fits of $\rho(E,\theta,X)$ have been found to be very useful for computational purposes. Fit over X of the form

$$\rho(E,\theta,X) = e^{\sum_{i=1}^{N} A_i X^{i-1}} \qquad (19)$$

has been found to give satisfactory results for normal incidence and half-space isotropic incidence, two cases of special interest. Fits of the above form were made and then the coefficients were fit as a function of energy. For normal incidence the coefficients are given by

$$\begin{aligned} A_1 &= 0.913\,e^{0.963E} + 0.021E + 0.215 \\ A_2 &= 5.0 - 0.491E \\ A_3 &= 57.573\,(E - 5.0)/(E + 29.98) \\ A_4 &= -1.6E^{0.837} \quad , \end{aligned} \qquad (20)$$

and for half-space isotropic the coefficients are given by

$$A_1 = 0.52 + 0.09854\,E^{-1.468}$$

$$A_2 = e^{-0.821E} - 1.0$$

$$A_3 = -2.5\left(e^{-1.022E} + 1.0\right)$$

$$A_4 = 3.253\,e^{-0.323E} + 5.8$$

$$A_5 = -15.4375 + 1.5542E - 0.0786077E^2 \quad . \tag{21}$$

Because the shape of the energy deposition function for angles near 90 deg is different from that near 0 deg, a good fit by a single functional form is difficult to achieve over the whole range of directions. Best results will probably be obtained by interpolation from the actual data or a smoothed set derived from it. The function $f(E,\theta,X)$ derived using the reflection and transmission factors was also fit but by a different form. The fit was to the form

$$1 - T_E(E,\theta,X) - A_E(E,\theta,X) = A\left[1 - e^{(BX + CX^2 + DX^3)}\right] \quad , \tag{22}$$

where A, B, C, and D are functions of E and θ. Then, taking the derivative with respect to X and using equation (14) yields

$$f(E,\theta,X) = -A\,(B + 2CX + 3DX^2)\,e^{(BX + CX^2 + DX^3)} \quad . \tag{23}$$

In Appendix F the terms A, B, C, and D are tabulated as a function of E and θ. Fits have been derived for the two cases of special interest. For a normally incident beam ($\theta = 0$ deg) in the energy range 0.5 to 10.0 MeV,

$$A = \frac{0.893 + 1.682E}{1.0 + 1.665E}$$

$$B = \frac{11.0E}{11.0E + 6.0} \tag{24}$$

$$C = 4.2\exp(-0.47E)$$

and

$$D = 5.16 \quad .$$

Berger has published a transmission and reflection coefficient for a cosine law source (half-space isotropic flux) [4]. In this case $f_{iso}(E,X)$ is a relatively insensitive function of E, and satisfactory results are obtained by taking an average curve for all energies. For energy deposition,

$$\begin{aligned} A &= 0.439 \\ B &= -2.08 \\ C &= -3.54 \\ D &= -6.08 \quad . \end{aligned} \tag{25}$$

The electron pathlength $r_0(E)$ in aluminum taken from Berger [3] has also been fit by the following form:

$$r_0(E) = (1.33 - 0.019E)\left(\sqrt{0.2713E^2 + 0.0121} - 0.11\right) , \tag{26}$$

which is within about 2 percent of actual curves for energies greater than 0.3 MeV and within 5 percent between 0.2 and 0.3 MeV.

ELECTRON TRANSPORT USING THE STRAIGHT-AHEAD AND CONTINUOUS SLOWING DOWN APPROXIMATIONS

A method commonly used for describing the transport of protons is to assume that the particle travels through the shield along its incident direction losing energy continuously according to some stopping power law. Thus, according to the approximations, the energy and direction of the particle at any point in the shield is completely predictable. This method has the advantage of providing an energy spectrum at the internal point of interest that may be used to determine such things as secondary production sources as well as to calculate dose deposition. Its disadvantages for application to electron transport are twofold: First, electrons are more likely to be scattered from their original direction than protons, and second, electrons can suffer large energy losses in a single interaction. Thus the straight-ahead approximations should not be expected to be especially applicable. The approximations have been applied with some success, however.

Since the validity of the approximations in applications to electron transport are somewhat questionable one would prefer to be on the conservative side in any estimate of particle energy or number. By using the extrapolated electron range rather than the mean range[3] for definition of other required quantities this can be accomplished. The extrapolated range is defined as shown in Figure 2, where it can be seen that few electrons penetrate beyond this distance. A very good fit to the extrapolated range in aluminum is given by

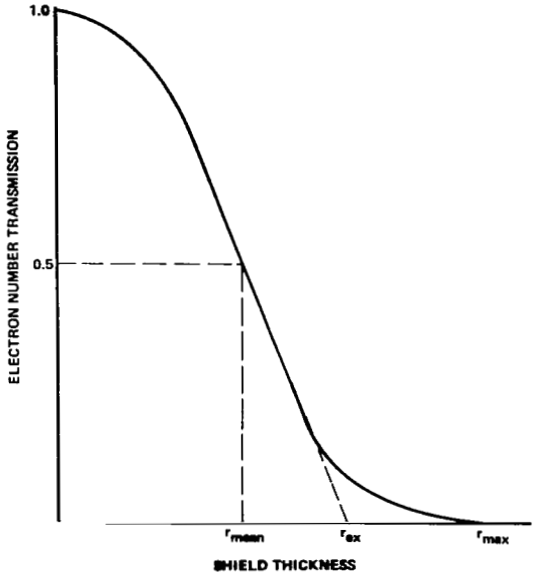

Figure 2. Definitions of electron mean range r_{mean}, extrapolated range r_{ex}, and maximum range r_{max}.

$$r_{ex} = R(E) = \sqrt{\frac{E^2}{a} + b^2} - b \quad (27)$$

over the energy range from 0.0 to 16.0 MeV. For $R(E)$ in g/cm^2, E is in MeV, a is 1.92, and b is 0.11 [6].

Given the electron range, one can determine the relationship between the initial energy and the energy after passing through thickness Z of material as follows:

Since

$$R(E) = R(E') + Z \quad , \quad (28)$$

where E is the initial energy and E' is the energy at depth Z,

$$E = g(E', Z) = R^{-1}[R(E') + Z)]; \quad (29)$$

R^{-1} denotes the inverse of the function R. Thus, using equations (27) and (29) gives

$$E = g(E', Z) = a\sqrt{\left[\sqrt{\left(\frac{E'}{a}\right)^2 + b^2} + Z\right]^2 - b^2} \quad . \quad (30)$$

3. This mean range is not Berger's mean pathlength [3].

The relationship between the external differential flux $\Phi_0(E)$ and the flux at depth Z, $\Phi_z(E')$, is given by

$$\Phi_z(E') = \Phi_0\,[g(E', Z)]\,\frac{dg(E', Z)}{dE'} \quad . \tag{31}$$

The derivative enters the equation because of change of energy to E' units; or as one can see, lower energy electrons lose energy faster, thus changing particle densities. Using equation (30) gives

$$\frac{dg(E', Z)}{dE'} = \frac{E'\left[\sqrt{\left(\frac{E'}{a}\right)^2 + b^2} + Z\right]}{a\sqrt{\left(\frac{E'}{a}\right)^2 + b^2}\ \sqrt{\left[\sqrt{\left(\frac{E'}{a}\right)^2 + b^2} + Z\right]^2 - b^2}} \quad . \tag{32}$$

The electron dose deposited at depth Z is given by

$$D(Z) = K \int_E \Phi_z(E')\, S(E')\, dE' \quad , \tag{33}$$

where $S(E')$ is the instantaneous collision stopping power in the receiver. One can derive an approximation for the stopping power by using the derivative of the range

$$S(E') = -\frac{1}{\frac{dR(E')}{dE'}} \quad . \tag{34}$$

Thus, using equation (27),

$$S(E') = \frac{a^2}{E'}\sqrt{\left(\frac{E'}{a}\right)^2 + b^2} \quad . \tag{35}$$

By a fortunate accident the approximate stopping power derived from aluminum extrapolated range data is a good fit to tissue collision stopping power. (Tissue is the receiver most commonly used.) The fit is within 5 percent of Berger's tabulated data [3] in the interval 0.15 to 4.5 MeV and within 13 percent from 0.08 to 10.0 MeV.

Combining the results of equations (31), (32), (33), and (35) and simplifying the tissue dose behind an aluminum shield Z thick yields

$$D(Z) = K \int_{E'} \Phi_0\left[g(E', Z)\right] \frac{a\left[\sqrt{\left(\frac{E'}{a}\right)^2 + b^2} + Z\right]}{g(E', Z)} \, dE' \quad . \tag{36}$$

Equation (36) is derived for normal incidence. For a beam incident at angle θ to the normal, Z is replaced in the equation by the slant distance to the dose point, $Z/\cos\theta$, and for half-space isotropic flux the dose is given by

$$D_{iso}(Z) = K \int_0^{\frac{\pi}{2}} \int_{E'} \Phi_0\left[g(E', Z/\cos\theta)\right] \frac{a\left[\sqrt{\left(\frac{E'}{a}\right)^2 + b^2} + Z/\cos\theta\right]}{g(E', Z/\cos\theta)} \, dE' \sin\theta \, d\theta \tag{37}$$

CALCULATIONS FOR SHIELD MATERIALS OTHER THAN ALUMINUM

One of the main weaknesses of the methods described for electron dose and spectral calculation described is that the shield material in all cases has been aluminum. Obviously it would be nice to have results from Berger's program for several materials covering the whole range of atomic numbers, but this would be an expensive calculation. For the straight-ahead approximation extrapolated range data are not available over the whole energy range for other materials. Until a more extensive set of data becomes available the approximation of replacing the shielding material by an aluminum shield of equivalent electron density can be used. This can be done for the calculations using Berger's data by replacing the pathlength $r_0(E)_{Al}$ by the expression

$$r_0(E) = \frac{Z_{Al}\, A}{Z\, A_{Al}} \, r_0(E)_{Al} = 0.481 \frac{A}{Z} \, r_0(E)_{Al} \quad , \tag{38}$$

where $r_0(E)$ is the pathlength in the original shielding material, A is its atomic weight, Z is its atomic number, and $r_0(E)_{Al}$ is the pathlength in aluminum. Figure 3 shows the ratio of $r_0(E)/r_0(E)_{Al}$ from Berger's tabulation [3] compared to the results from equation (38). As can be seen, for material near aluminum in atomic number the approximation is fairly good. For the straight-ahead calculation the approximation is more easily made by replacing the shield thickness by a thickness of aluminum given by

$$X_{Al} = \frac{A_{Al}\, Z}{Z_{Al}\, A}\, X \qquad (39)$$

$$= 2.08\, \frac{Z}{A}\, X \quad ,$$

where X is the original shield thickness in g/cm^2.

COMPARISON OF THE THREE METHODS FOR DOSE CALCULATION

Typical electron spectra encountered in practical applications are exponential in nature. Figures 4 through 9 show comparisons of the three methods for spectra of the form

$$\Phi_0(E) = Pe^{-PE} \quad , \qquad (40)$$

where P varies from 0.25 to 6.0. The energy integration limits are 0.0 to 20.0 MeV. The agreement among the three methods is fairly good considering the magnitude of the attenuation that occurs. The two methods using Berger's data have significant disagreement only for high shield thicknesses and isotropic spectra. The disagreement here is probably because a significant fraction of the dose is from electrons with energies above 10 MeV where both methods are using extrapolation on the data. The disagreement between the methods using Berger's data and the straight-ahead method are somewhat larger, but the errors still are not so large as to cause question about the validity of any one of the three approaches.

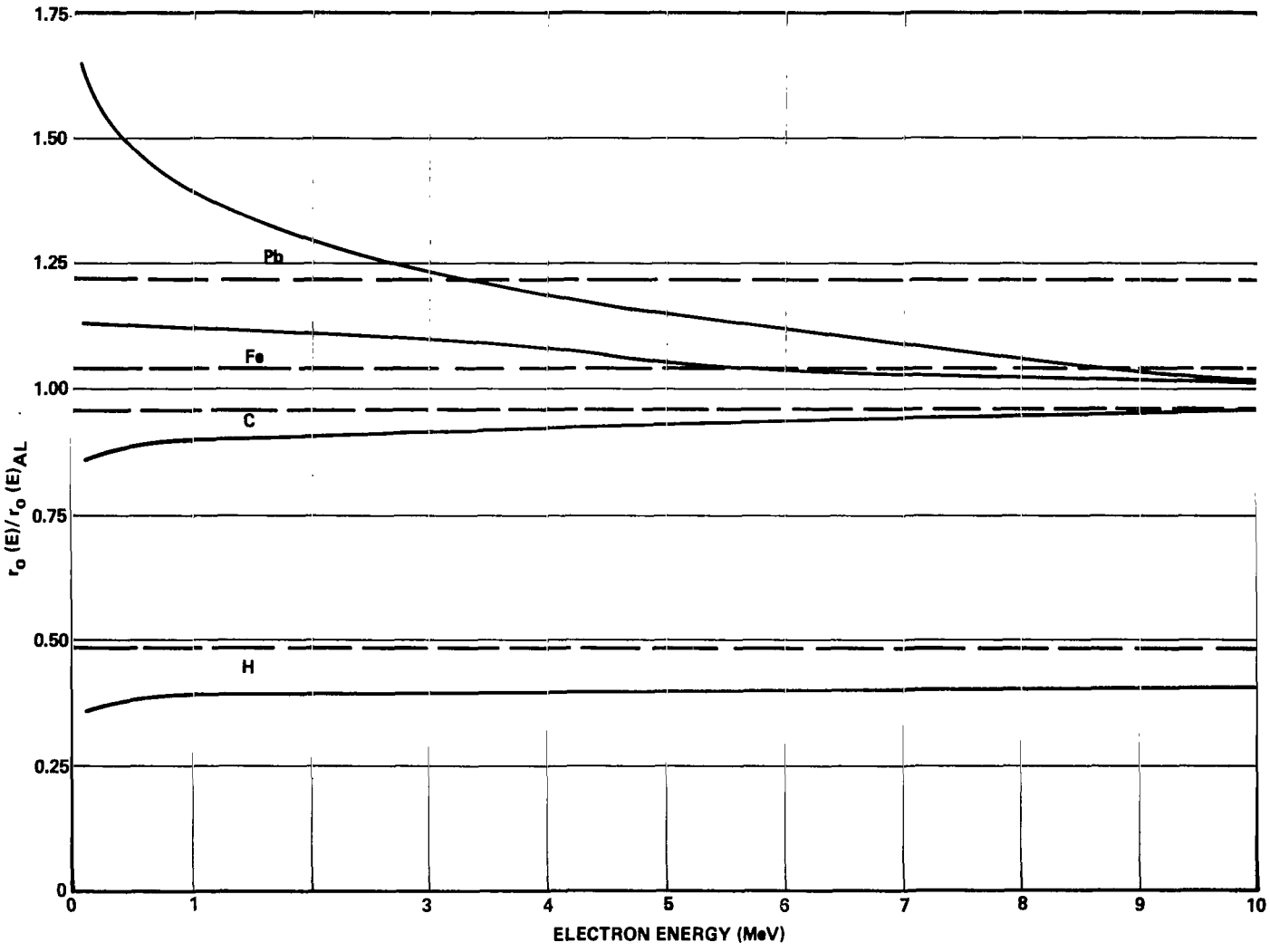

Figure 3. Ratios of lead, iron, carbon, and hydrogen pathlengths to pathlength in aluminum as a function of energy.

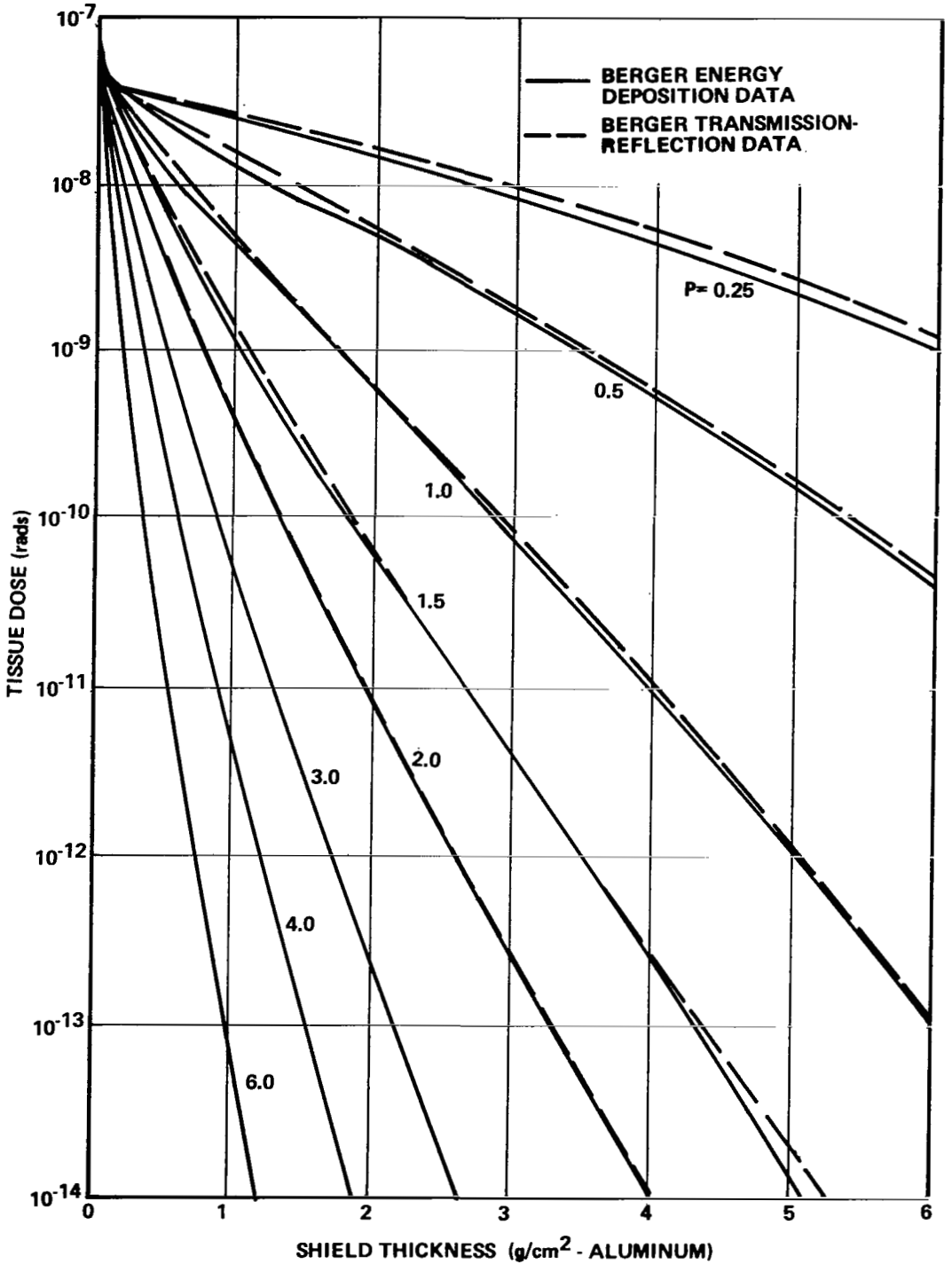

Figure 4. Comparison of electron tissue doses calculated using Berger's energy deposition data and transmission—reflection data for a normally incident spectrum of the form $\Phi_0(E) = P \exp(-PE)\, e/cm^2$ - MeV.

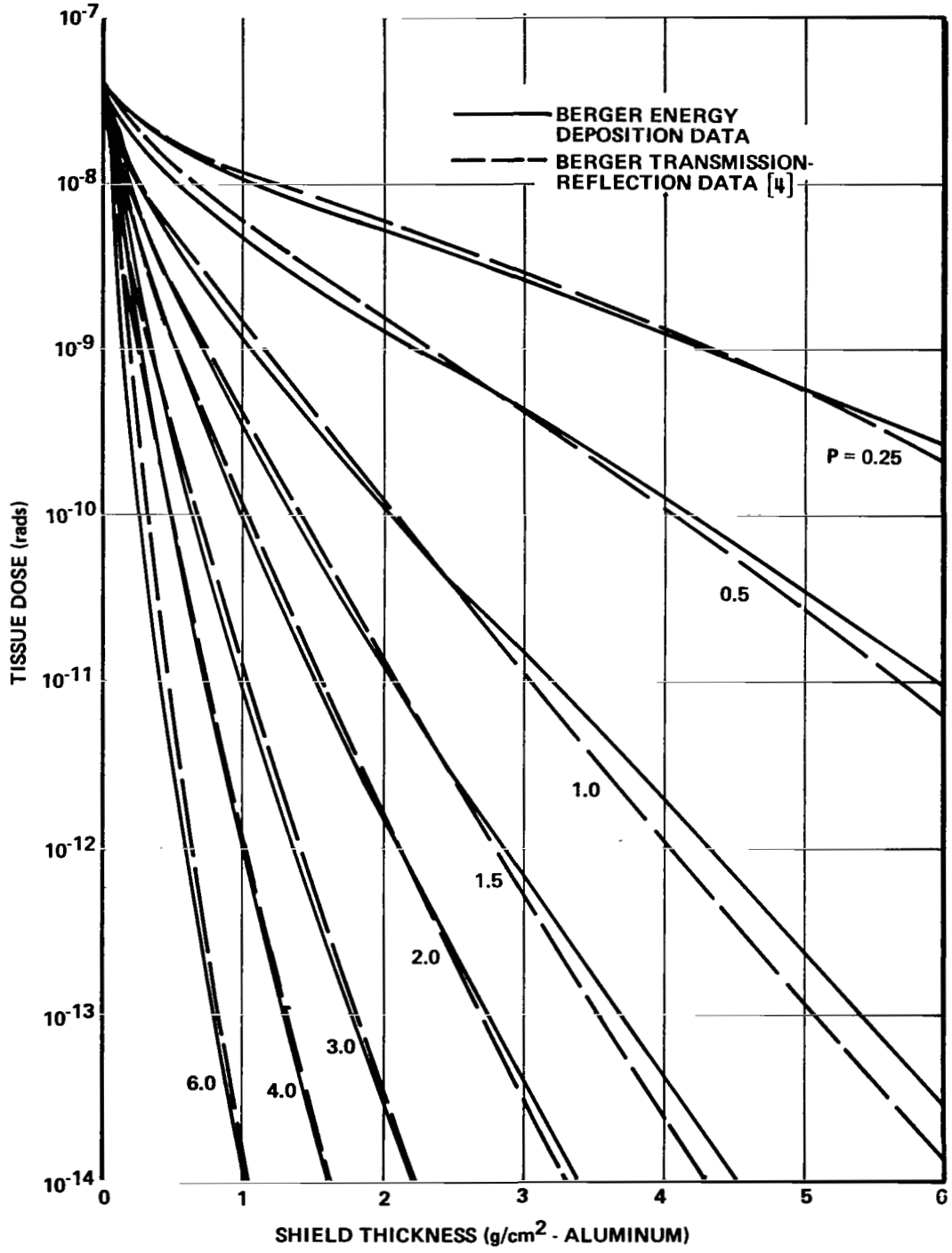

Figure 5. Comparison of electron tissue doses calculated using Berger's energy deposition data and transmission—reflection data for a half-space isotropic incident spectrum of the form $\Phi_0(E) = P \exp(-PE)$ e/cm^2 - MeV.

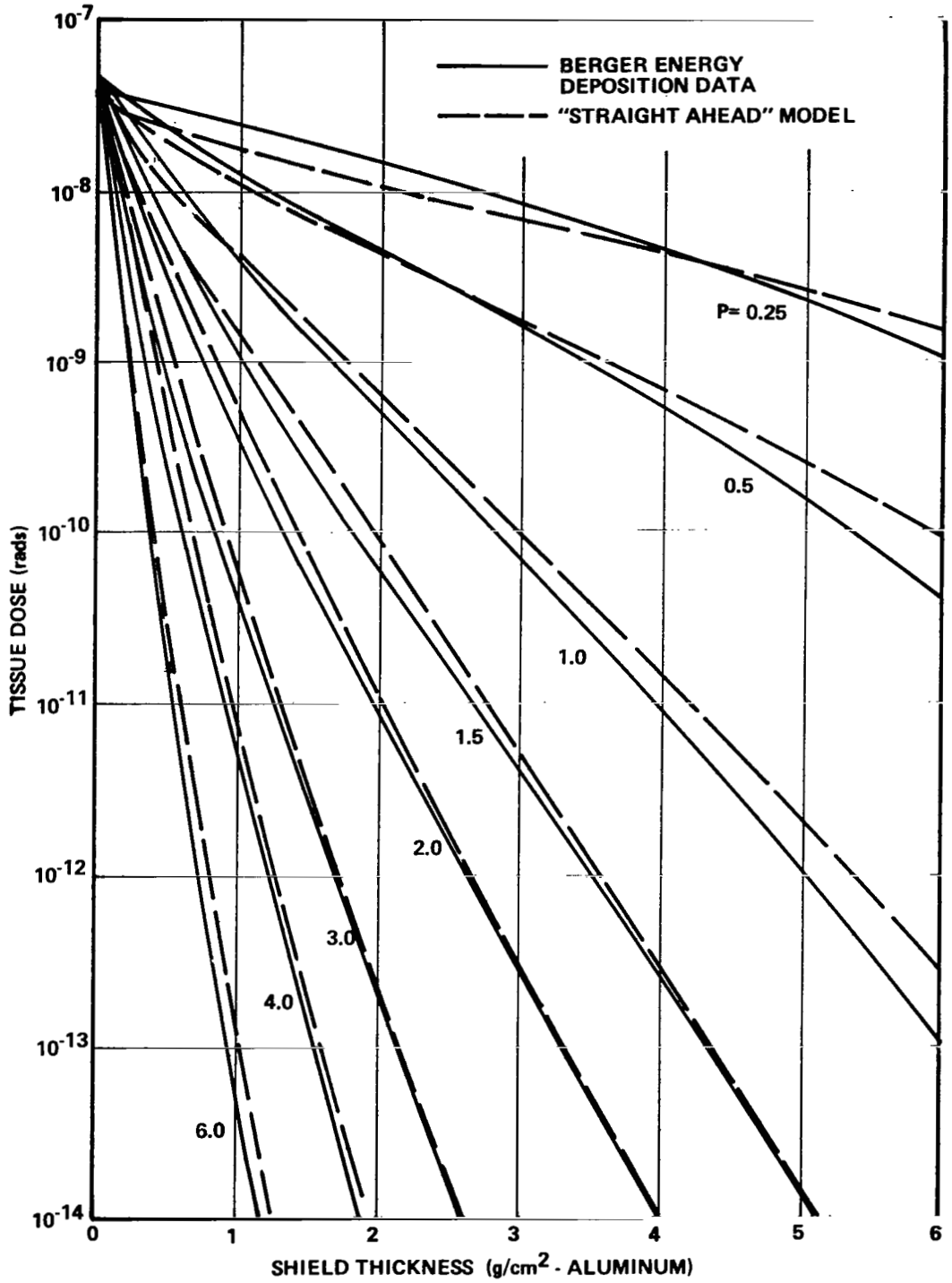

Figure 6. Comparison of electron tissue doses calculated using Berger's energy deposition data and the straight-ahead model for a normally incident spectrum of the form $\Phi_0(E) = P \exp(-PE)$ e/cm^2 - MeV.

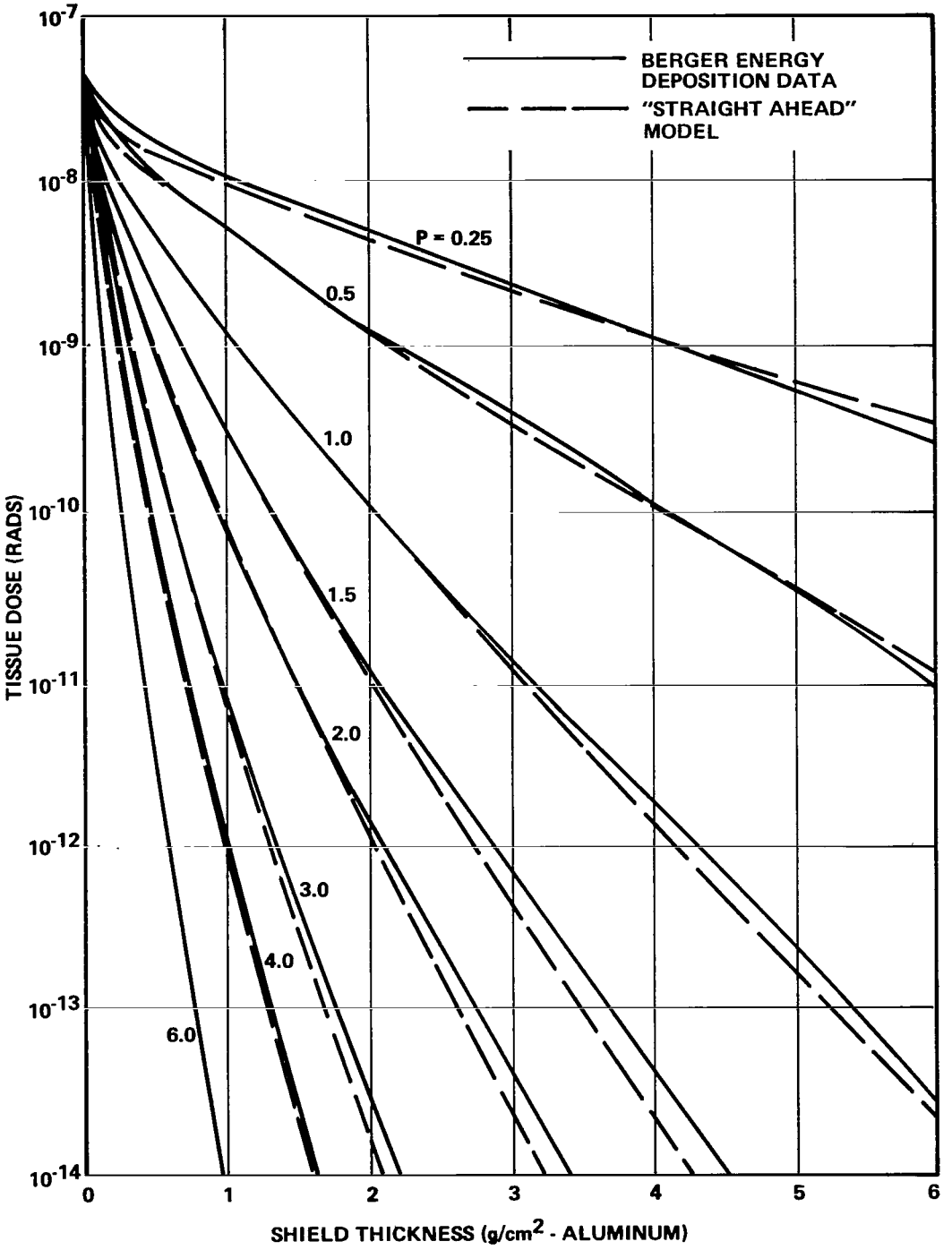

Figure 7. Comparison of electron tissue doses calculated using Berger's energy deposition data and the straight-ahead model for a half-space isotropic incident electron spectrum of the form $\Phi_0(E) = P \exp(-PE)\ e/cm^2 - MeV$.

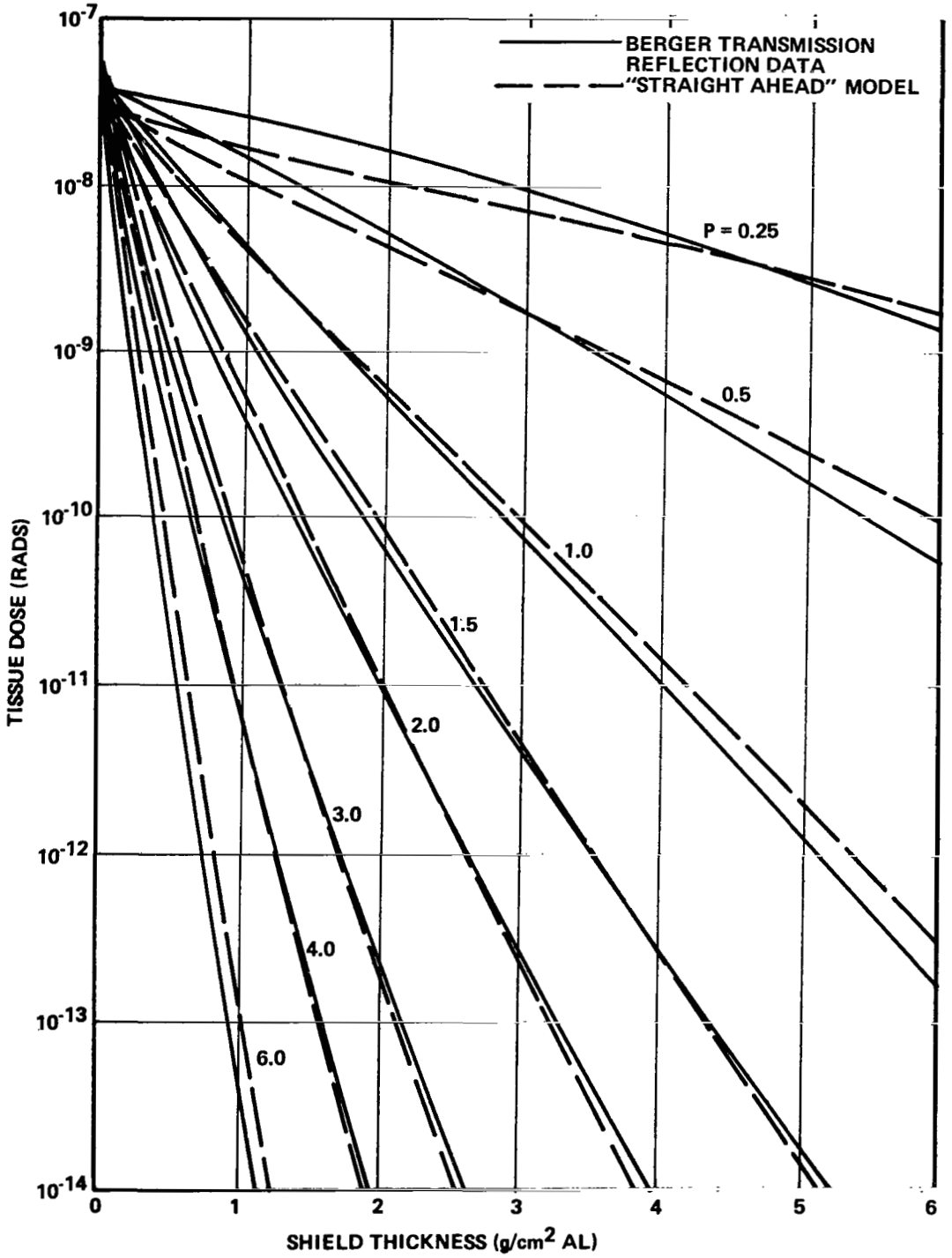

Figure 8. Comparison of electron tissue doses calculated using Berger's transmission—reflection data and the straight-ahead model for a normally incident spectrum of the form $\Phi_0(E) = P \exp(-PE)$ e/cm^2 - MeV.

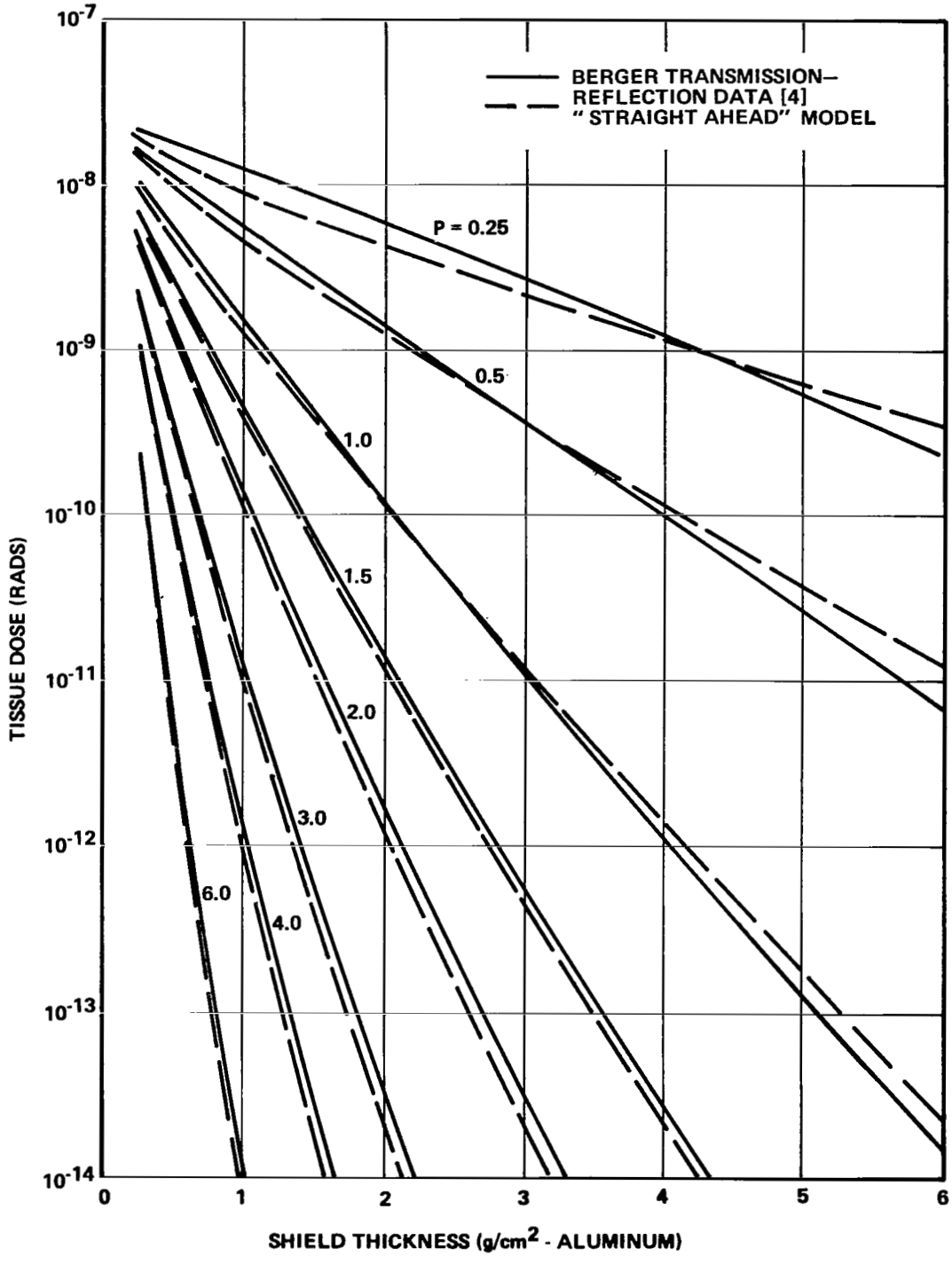

Figure 9. Comparison of electron tissue doses calculated using Berger's transmission—reflection data and the straight-ahead model for a half-space isotropic incident spectrum of the form $\Phi_0(E) = P \exp(-PE)\, e/cm^2$ - MeV.

BREMSSTRAHLUNG DOSE CALCULATIONS

Previously, consideration has been confined to the dose deposited by electrons; this is satisfactory for thin shields. However, when the shields are thick enough to remove a large fraction of the primary electrons, dose deposition by bremsstrahlung must be taken into account. (The point where this occurs is usually less than 3.0 g/cm^2.) To do a bremsstrahlung dose calculation one must generate a bremsstrahlung source distribution and then transport the bremsstrahlung from this source to the dose point. To generate the bremsstrahlung source distribution one needs the electron energy and angular distribution at the source point and the bremsstrahlung production cross section.

Because the interior electron angular distribution is not easily determined and since the bremsstrahlung production cross section differentials in angle are not particularly accurate, a simplification commonly made is to use cross section differential in photon energy only and to make some assumption about the bremsstrahlung source angular distribution. (This assumption will be examined later.) In this case the bremsstrahlung differential energy flux source or depth Z' and photon energy E_γ is given by

$$S(E_\gamma, Z') = \int_E \int_{\vec{\Omega}} E_\gamma \sum (E_\gamma, E)\, \Phi_{Z'}(E, \vec{\Omega})\, dE\, d\vec{\Omega} \qquad (41)$$

in units of MeV/(MeV-g), where $\sum (E_\gamma, E)$ is the macroscopic bremsstrahlung production cross section differential in photon energy in units of $\frac{\text{photons}}{\text{g-MeV-(e/cm}^2\text{)}}$ and $\Phi_{Z'}(E,\vec{\Omega})$ is the electron energy and angular distribution at depth Z in units of $\frac{e}{\text{cm}^2\text{-MeV-sr}}$.

The macroscopic cross section is given by

$$\sum (E_\gamma, E) = \frac{N_0}{A} \frac{d\sigma}{dE_\gamma} , \qquad (42)$$

where N_0 is Avagadro's number 6.02×10^{23} atom/mole, A is the atomic weight of the material at the source point in g/mole, and $\frac{d\sigma}{dE}$ is the microscopic bremsstrahlung production cross section differential in photon energy in units of $\frac{\text{photons}}{\text{atom} \cdot (e/cm^2) \cdot \text{MeV}}$. The microscopic cross section presently used for the MSFC calculation is given by

$$\frac{d\sigma}{dE_\gamma} = F_E(E, E_\gamma)\, C(E)\, \frac{Z_0^2 r_0^2 P}{137 E_\gamma P_0} \left(\frac{4}{3} - 2H_0H\left(\frac{P^2 + P_0^2}{P^2 P_0^2}\right) + \frac{\epsilon_0 H}{P_0^3} + \frac{\epsilon H_0}{P^3} - \frac{\epsilon \epsilon_0}{P_0 P} + L \left\{ \frac{8 H_0 H}{3 P_0 P} + \frac{K^2 (H_0^2 H^2 + P_0^2 P^2)}{P_0^3 P^3} + \frac{K}{2 P_0 P} \left[\left(\frac{H_0 H + P_0^2}{P_0^3}\right) \epsilon_0 - \left(\frac{H_0 H + P^2}{P_3}\right) \epsilon + \frac{2 K H_0 H}{P^2 P_0} \right] \right\} \right) , \quad (43)$$

where

$$L = 2 \ell n \left(\frac{H_0 H + P_0 P - 1}{K} \right)$$

$$\epsilon_0 = \ell n \left(\frac{H_0 + P_0}{H_0 - P_0} \right)$$

$$\epsilon = \ell n \left(\frac{H + P}{H - P} \right) .$$

The terms H_0 and H are the initial and final total electron energies in mc^2 units given by

$$H_0 = \frac{E}{mc^2} + 1$$

$$H = \frac{E - E_\gamma}{mc^2} + 1 \quad ;$$

P_0 and P are the initial and final electron momenta given by

$$P_0 = \sqrt{H_0^2 - 1}$$

$$P = \sqrt{H^2 - 1} \quad ;$$

and K is the photon energy or momentum in mc^2 or mc units, respectively,

$$K = \frac{E_\gamma}{mc^2} \quad .$$

The term Z_0 is the atomic number of the source material, r_0 is the classical electron radius 2.82×10^{-13} cm, mc^2 is the rest mass energy of an electron, and $F_E(E, E_\gamma)$ and $C(E)$ are two correction factors. Except for the correction factors this is formula 3BN from Koch and Motz [7], who give a complete description of the cross section. The correction factor $F_E(E, E_\gamma)$ given by

$$F_E(E, E_\gamma) = \begin{cases} \dfrac{\beta_0 \left(1 - e^{\frac{2\pi Z_0}{137\beta_0}}\right)}{\beta \left(1 - e^{\frac{2\pi Z_0}{137\beta}}\right)} & \text{for } E < 2.0 \text{ MeV} \\ & \quad \dfrac{E_\gamma}{E} > 0.01 \\ 1.0 & \text{otherwise} \end{cases} \quad , \qquad (44)$$

where

$$\beta_0 = \sqrt{1 - \left(\frac{mc^2}{E + mc^2}\right)^2} \tag{45}$$

and

$$\beta = \sqrt{1 - \left(\frac{mc^2}{E - E_\gamma + mc^2}\right)^2} \quad , \tag{46}$$

is the Elwert nonrelativistic coulomb correction, and the correction C(E) is an empirical screening correction as shown by Koch and Motz [7]. (Appendix G is a tabulation of results read from the graph.) Koch and Motz further discuss both these corrections [7].

The prime advantage of the straight-ahead approximation is that it does provide an electron spectrum at a given depth. Thus, using the result derived, for a normally incident electron beam the bremsstrahlung source is given as

$$S_N(E_\gamma, Z') = \int_E E_\gamma \sum(E_\gamma, E)\, \Phi_0\, [g(E, Z')]\, \frac{dg(E, Z')}{dE}\, dE \quad , \tag{47}$$

and for a half-space isotropic incident electron distribution the bremsstrahlung source is

$$S_{iso}(E_\gamma, Z') = \int_0^{\frac{\pi}{2}} \int_E E_\gamma \sum(E_\gamma, E)\, \Phi_0\, g(E, Z'/\cos\theta)\, \frac{dg(E, Z'/\cos\theta)}{dE}\, dE \sin\theta\, d\theta \quad , \tag{48}$$

where Φ_0, g, and $\frac{dg}{dE}$ are as defined in the fourth section.

The bremsstrahlung transport and dose calculation is relatively straightforward for a plane slab geometry given the source energy distribution and some source angular distribution. Using point kernel attentuation with dose buildup factors, the dose is given by

$$D(Z) = K \int_{E_\gamma} \int_0^Z \mu_E(E_\gamma)\, S(E, Z')\, B(E_\gamma, Z, Z')\, G[\mu_m(E_\gamma)|Z - Z'|]\, dE_\gamma\, dZ' \quad , \tag{49}$$

where $\mu_E(E_\gamma)$ is the gamma ray energy absorption coefficient [8] for the receiver material; Z is the shield thickness; $B(E, Z, Z')$ is a dose buildup factor, depending on the source angular distribution chosen; and $G[\mu_m(E_\gamma)|Z-Z'|]$ is the attenuation kernel, also depending on the source angular distribution chosen where $\mu_m(E_\gamma)$ is the gamma ray mass absorption coefficient.

Much of the wide disagreement among various bremsstrahlung calculations can be traced to assumptions made about either the incident electron angular distribution expected in the problem or the angular distribution of the bremsstrahlung source. Perhaps the least conservative assumption about the source distribution that can logically be made for deep penetrations is that it is isotropic, and the most conservative assumption is that all the photons are emitted normally into the slab. In the first case the attenuation kernel is given by

$$G[\mu_m(E_\gamma)\,|Z-Z'|] = \frac{E_1\,[\mu_m(E_\gamma)|Z-Z'|]}{2}\quad , \tag{50}$$

where E_1 is the first exponential integral and plane isotropic buildup factors are used [9]. In the second case the attenuation kernel is

$$G[\mu_m(E_\gamma)\,|Z-Z'|] = e^{-\mu_m(E_\gamma)\,|Z-Z'|}\quad , \tag{51}$$

and plane monodirectional buildup factors are used. Goldstein [8] tabulates these for infinite media, which should give a conservative estimate of the dose. These should be used cautiously, however, because they do not extend low enough in energy and extrapolation is dangerous. Figure 10 gives a comparison of these two cases for a half-space isotropic electron spectrum of exponential form incident on an aluminum shield with a water receiver (simulating tissue). Plane isotropic buildup factors were used in both calculations so that the difference observed is caused by the attenuation kernel. Actually, if correct buildup factors were used, the normal incident source case would be slightly lower.

Because of the built-in bias of using the extrapolated range in the straight-ahead approximation for calculating the source distribution it is felt that there is no need to use the most conservative source angular distribution. Instead it is assumed that the bremsstrahlung source is half-space isotropic

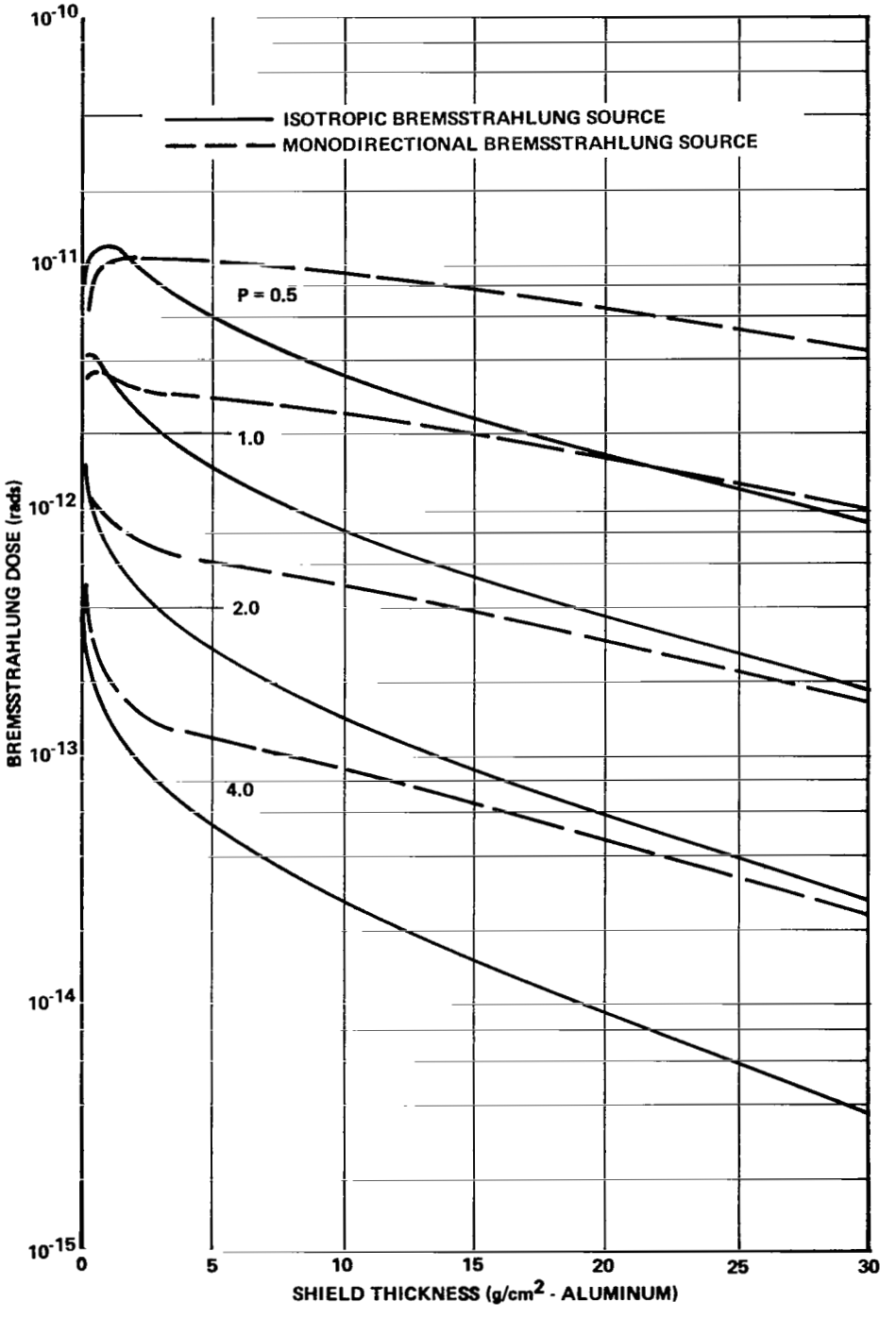

Figure 10. Comparison of bremsstrahlung dose calculated assuming an isotropic source and a monodirectional source directed normally inward for a half-space isotropic incident electron spectrum of the form $\Phi_0(E) = P \exp(-PE)$ e/cm^2 MeV.

toward the receiver by the attenuation function given in equation (50) multiplied by a factor of two. Still, the plane isotropic buildup factors [9] are used, making the calculation slightly more conservative. Figure 11 shows the results of an MSFC bremsstrahlung calculation for a half-space isotropic electron spectrum of exponential form incident on an aluminum shield with a water receiver (simulating tissue). Comparing Figures 10 and 11 reveals that the MSFC calculation (Fig. 11) is the most conservative of the three up to 4 or 5 g/cm^2. Above that depth, the monodirectional source calculation is more conservative by as much as a factor of three compared to the MSFC results.

Since the bremsstrahlung dose calculational methods described so far involved triple or quadruple numerical integration and since the functions integrated are exceptionally difficult to integrate, the calculation can be performed conveniently only on a relatively large computer. In many cases, all that is needed is a rough order of magnitude estimate useful only in determining if a problem exists. For space applications, where most of the electron spectra encountered fall off exponentially with increasing energy, a conservative estimate of bremsstrahlung dose can be calculated as follows:

First, assume that all the electrons penetrate to the source plane and that at that plane their energy is the average energy of an external electron. That is,

$$\bar{E} = \frac{\int_{\vec{\Omega}} \int_{E'} E' \Phi_0 (E', \vec{\Omega}) \, dE' \, d\vec{\Omega}}{\int_{\vec{\Omega}} \int_{E'} \Phi_0 (E', \vec{\Omega}) \, dE' \, d\vec{\Omega}} \quad . \tag{52}$$

According to Evans [10], the total source in MeV/g is approximated by

$$S = H \, Z_0 \, \bar{E}^2 \int_{\vec{\Omega}} \int_{E'} \Phi_0 (E', \vec{\Omega}) \, dE' \, d\vec{\Omega} \quad , \tag{53}$$

where H is a constant and Z_0 is the shield material atomic number. Berger and Seltzer [4] tabulate H for a cosine law electron source as a function of incident electron energy and shield thickness. Because the variation in the table is not great, a typical value 4×10^{-4} can be used for this approximation.

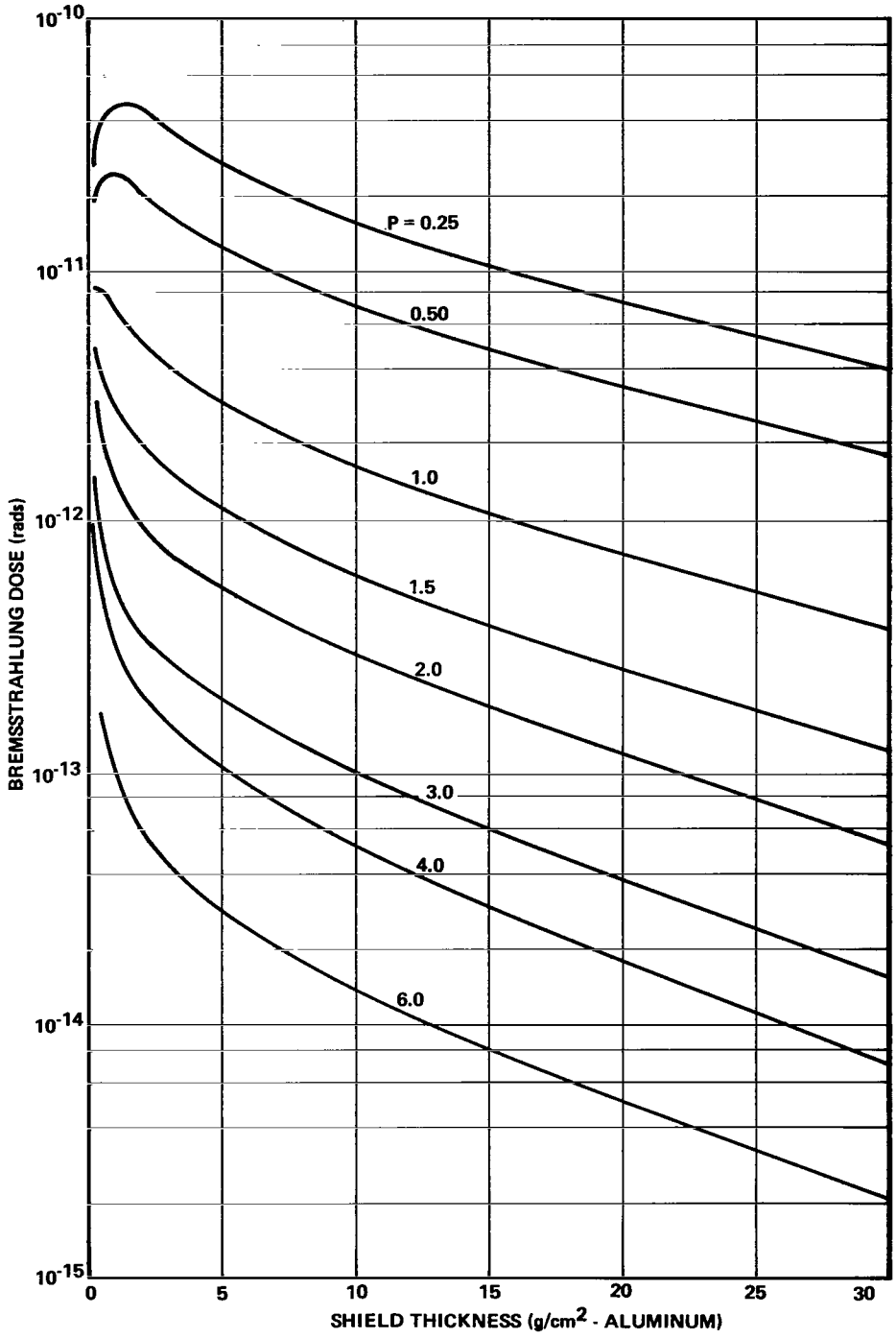

Figure 11. Bremsstrahlung dose calculations assuming a half-space isotropic source for a half-space isotropic incident electron spectrum of the form $\Phi_0(E) = P \exp(-PE)$ e/cm^2-MeV.

Second, assume that the source plane is located at half the extrapolated range at $\bar{E}$. The bremsstrahlung dose is given by

$$D(Z) = K \mu_E S B[\bar{E}, \mu_m(\bar{E}) Z^*] E_1[\mu_m(\bar{E}) Z^*] \quad . \tag{54}$$

For μ_E, the energy absorption coefficient in the receiver, 0.033 cm^2/g is used, which is an upper bound on the coefficient for water in the range above 0.1 MeV. The source-receiver distance is given by

$$Z^* = Z - R(\bar{E})/2 \qquad Z > R(\bar{E})/2 \quad . \tag{55}$$

A rough fit of the buildup factor in aluminum is given by

$$B(\bar{E}, \mu_m(\bar{E}) Z^*) = \begin{cases} 1.0 + 26.47 \mu_m(\bar{E}) Z^* \bar{E}^{1.161} & \bar{E} < 0.1 \\ 1.0 + 1.827 \mu_m(\bar{E}) Z^* & 0.1 \le \bar{E} \le 0.2016 \\ 1.0 + 1.253 \mu_m(\bar{E}) Z^* \bar{E}^{-0.2354} & 0.2016 < E \le 2.0 \\ 1.0 + 1.528 \mu_m(\bar{E}) Z^* \bar{E}^{-0.522} & \bar{E} > 2.0 \quad . \end{cases} \tag{56}$$

Simplifying somewhat for an aluminum shield and a water receiver yields

$$D(Z) = 2.7 \times 10^{-12} \bar{E}^2 B[E, \mu_m(\bar{E}) Z^*] E_1[\mu_m(\bar{E}) Z^*] \int_{\bar{\Omega}} \int_{E'} \Phi_0(E', \vec{\Omega}) dE' d\vec{\Omega} \quad . \tag{57}$$

Figure 12 shows the result of a bremsstrahlung dose calculation using equation (57); Figure 13 shows a similar calculation assuming a monodirectional source. As can be seen in comparisons with results of more accurate calculations, the approximation yields reasonable order of magnitude estimates that are generally conservative.

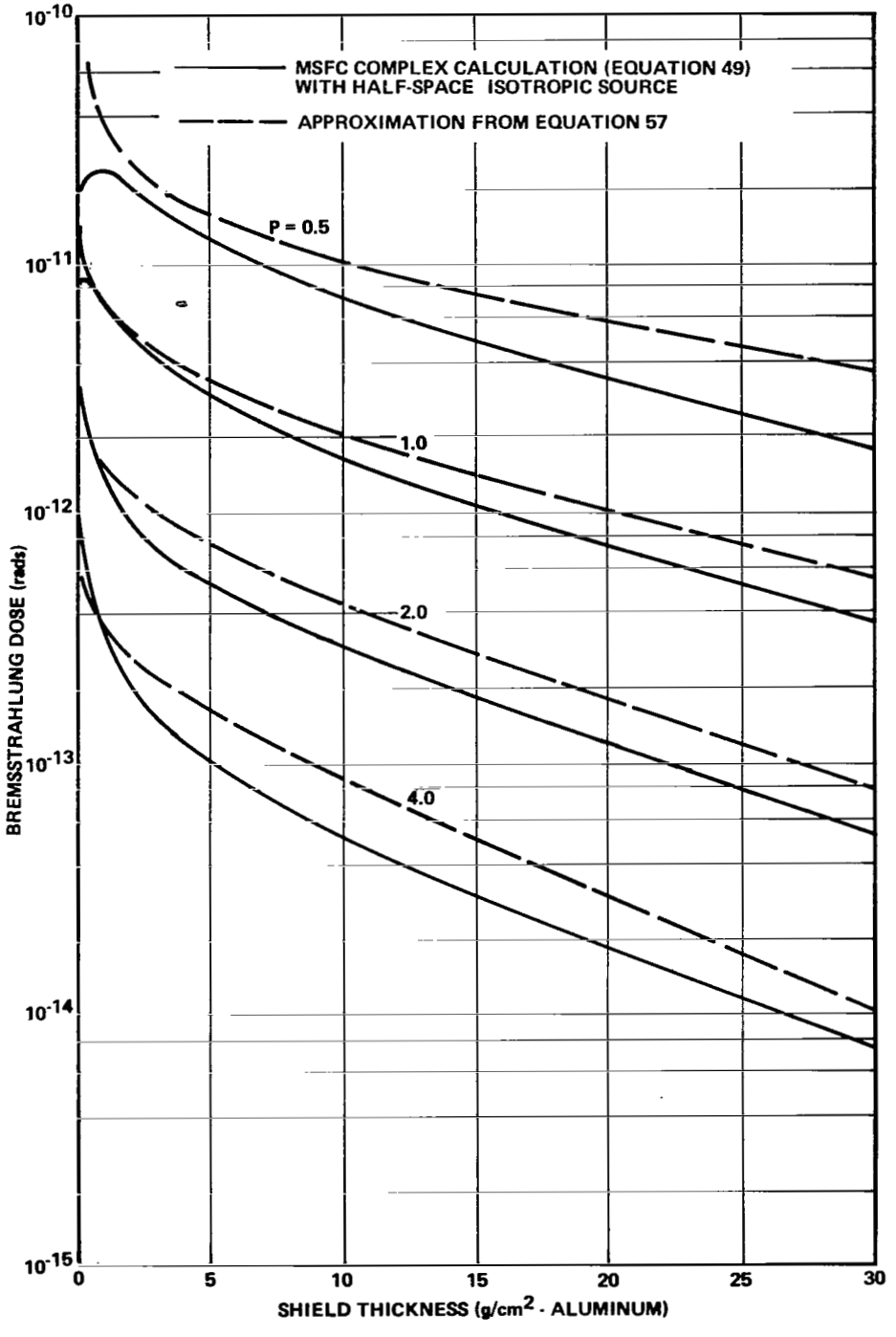

Figure 12. Comparison of bremsstrahlung doses calculated assuming a half-space isotropic source and incident spectrum in the complex MSFC calculation [equation (49)] and using equation (57). The spectrum is of the form $\Phi_0(E) = P \exp(-PE)$ e/cm^2-MeV.

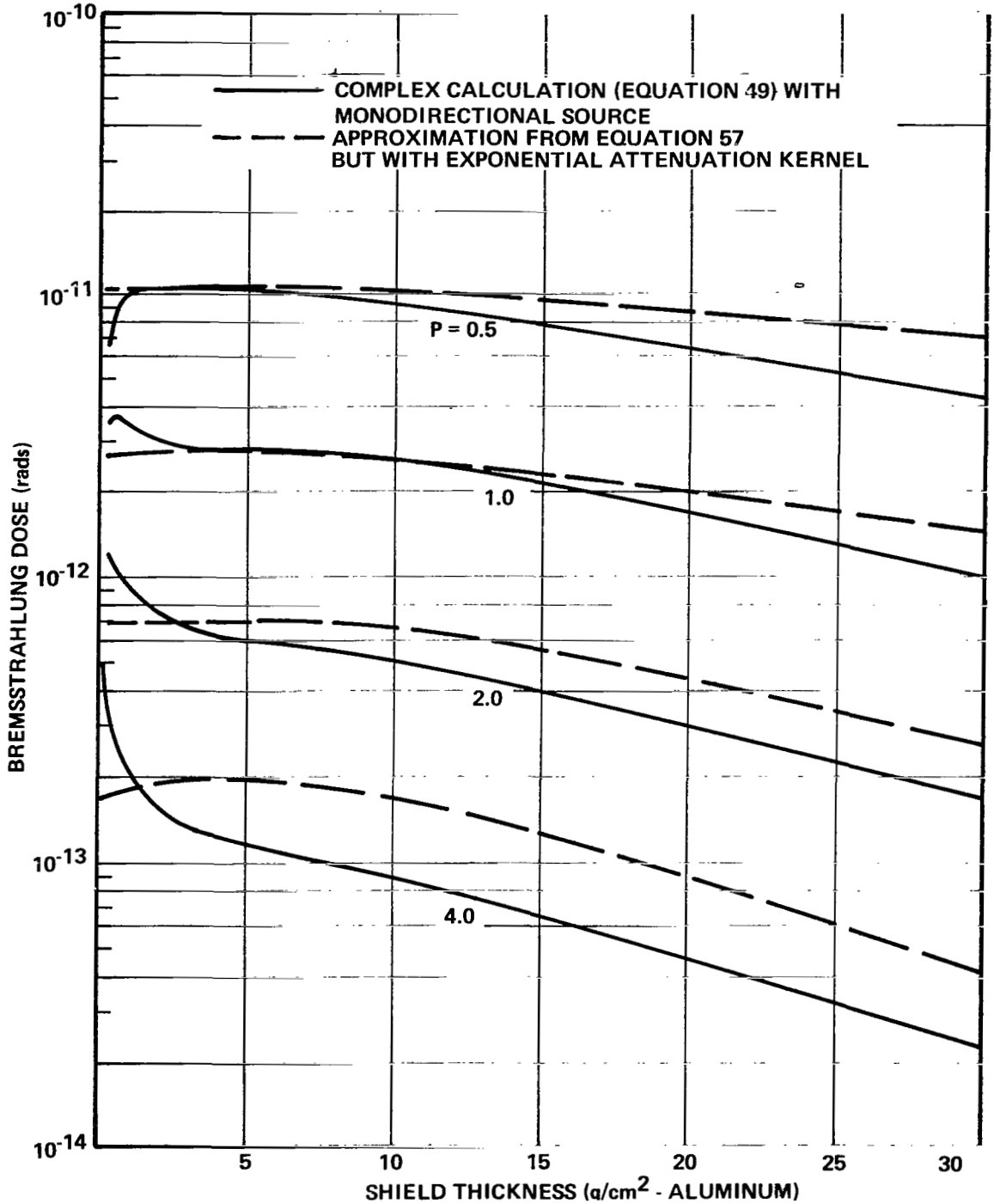

Figure 13. Comparison of bremsstrahlung dose calculated assuming a monodirectional source directed normally inward and a half-space isotropic electron spectrum of the form $\Phi_0(E) = P \exp(-PE)$ e/cm^2-MeV in the complex MSFC calculation [equation (49)] and using equation (57) but with an exponential attenuation kernel.

CONCLUSION

Although the results of the different electron and bremsstrahlung dose calculations developed at MSFC give results in relatively good agreement with each other, comparison with independent calculation is useful in pointing up areas of possible weakness. Wayne Scott of Oak Ridge National Laboratory has made such calculations using a Boeing program called Charge and a Douglas program called BEP as well as an older version of the MSFC program using Berger's transmission and reflection data [11]. The spectrum used was

$$\Phi_0(E) = 3.88\, e^{-0.575E-0.055E^2} \quad \frac{e}{cm^2\text{-MeV-sec}} \quad , \qquad (58)$$

which was renormalized to a total flux of unity. Table 2 gives the calculated electron dose in units of rad/h behind an aluminum shield on a tissue receiver for a normally incident beam. The MSFC results shown are for the new program using Berger's energy deposition coefficients and for the straight-ahead approximation. Both the MSFC program results are higher than the Charge and BEP results. The calculation using Berger's data is believed to be higher because the receiver had infinite backing behind it, whereas the other programs assume no backing. The straight-ahead calculation was higher because the extrapolated range was used in describing the transport.

Scott also did some spectral calculation at 0.5 and 1.0 g/cm^2 for the same incident spectrum using Charge, BEP, and Berger's Monte Carlo program ETRAN. Figures 14 and 15 show these results plus spectra calculated with the MSFC straight-ahead program; it can be seen why the straight-ahead program yields higher doses. For the low-energy end of the spectrum consisting of particles that have lost the largest fraction of their energy and been scattered the most, the straight-ahead program overestimates the flux by as much as a factor of three compared to ETRAN. For higher energies there is relatively good agreement with ETRAN. The overestimate of the low-energy component of the electron flux will be reflected in the bremsstrahlung calculation as an overestimate of the low-energy component of the bremsstrahlung source and in turn an overestimate of the bremsstrahlung dose, especially behind the thin shield where the low-energy bremsstrahlung has not been attenuated greatly.

In conclusion, the program using Berger's energy deposition data should be preferred for dose calculations, because in most practical problems

TABLE 2. ELECTRON TISSUE DOSE (rads/h) CALCULATED BY SEVERAL DIFFERENT PROGRAMS FOR A NORMALLY INCIDENT BEAM ON AN ALUMINUM SHIELD

Shield Thickness (g/cm^2)	McDonald Douglas Code: Charge	Boeing Electron Dose Code BEP	MSFC Berger Energy Deposition Electron Code	MSFC "Straight Ahead" Electron Code
0.0	1.11×10^{-4}		1.95×10^{-4}	1.65×10^{-4}
0.01	1.13×10^{-4}	1.48×10^{-2}	1.68×10^{-4}	1.30×10^{-4}
0.02	1.17×10^{-4}	1.24×10^{-4}	1.65×10^{-4}	1.23×10^{-4}
0.03	1.17×10^{-4}	7.99×10^{-5}	1.64×10^{-4}	1.18×10^{-4}
0.04	1.17×10^{-4}	7.42×10^{-5}	1.62×10^{-4}	1.15×10^{-4}
0.05	1.14×10^{-4}	5.48×10^{-5}	1.61×10^{-4}	1.12×10^{-4}
0.06	1.38×10^{-4}	5.27×10^{-5}	1.59×10^{-4}	1.10×10^{-4}
0.07	9.52×10^{-5}	7.10×10^{-5}	1.56×10^{-4}	1.07×10^{-4}
0.08	9.27×10^{-5}	4.47×10^{-5}	1.54×10^{-4}	1.05×10^{-4}
0.09	8.95×10^{-5}	4.32×10^{-5}	1.51×10^{-4}	1.03×10^{-4}
0.10	8.45×10^{-5}	4.13×10^{-5}	1.49×10^{-4}	1.01×10^{-4}
0.20	6.17×10^{-5}	3.01×10^{-5}	1.21×10^{-4}	8.58×10^{-5}
0.30	4.94×10^{-5}	2.30×10^{-5}	9.67×10^{-5}	7.35×10^{-5}
0.40	4.11×10^{-5}	1.77×10^{-5}	7.75×10^{-5}	6.29×10^{-5}
0.50	3.35×10^{-5}	1.39×10^{-5}	6.23×10^{-5}	5.38×10^{-5}
0.60	2.75×10^{-5}	1.09×10^{-5}	5.02×10^{-5}	4.59×10^{-5}
0.70	2.07×10^{-5}	8.59×10^{-6}	4.05×10^{-5}	3.90×10^{-5}
0.80	1.65×10^{-5}	6.80×10^{-6}	3.28×10^{-5}	3.31×10^{-5}
0.90	1.32×10^{-5}	5.40×10^{-6}	2.66×10^{-5}	2.79×10^{-5}
1.00	1.06×10^{-5}	4.29×10^{-6}	2.16×10^{-5}	2.35×10^{-5}
2.00	1.16×10^{-6}	4.25×10^{-7}	2.60×10^{-6}	3.43×10^{-6}
3.00	1.37×10^{-7}	2.80×10^{-8}	2.60×10^{-7}	3.44×10^{-7}
4.00	1.83×10^{-8}	0	1.97×10^{-8}	2.35×10^{-8}
5.00	1.10×10^{-9}	0	1.09×10^{-9}	1.12×10^{-9}
6.00	0	0	4.54×10^{-11}	4.73×10^{-11}

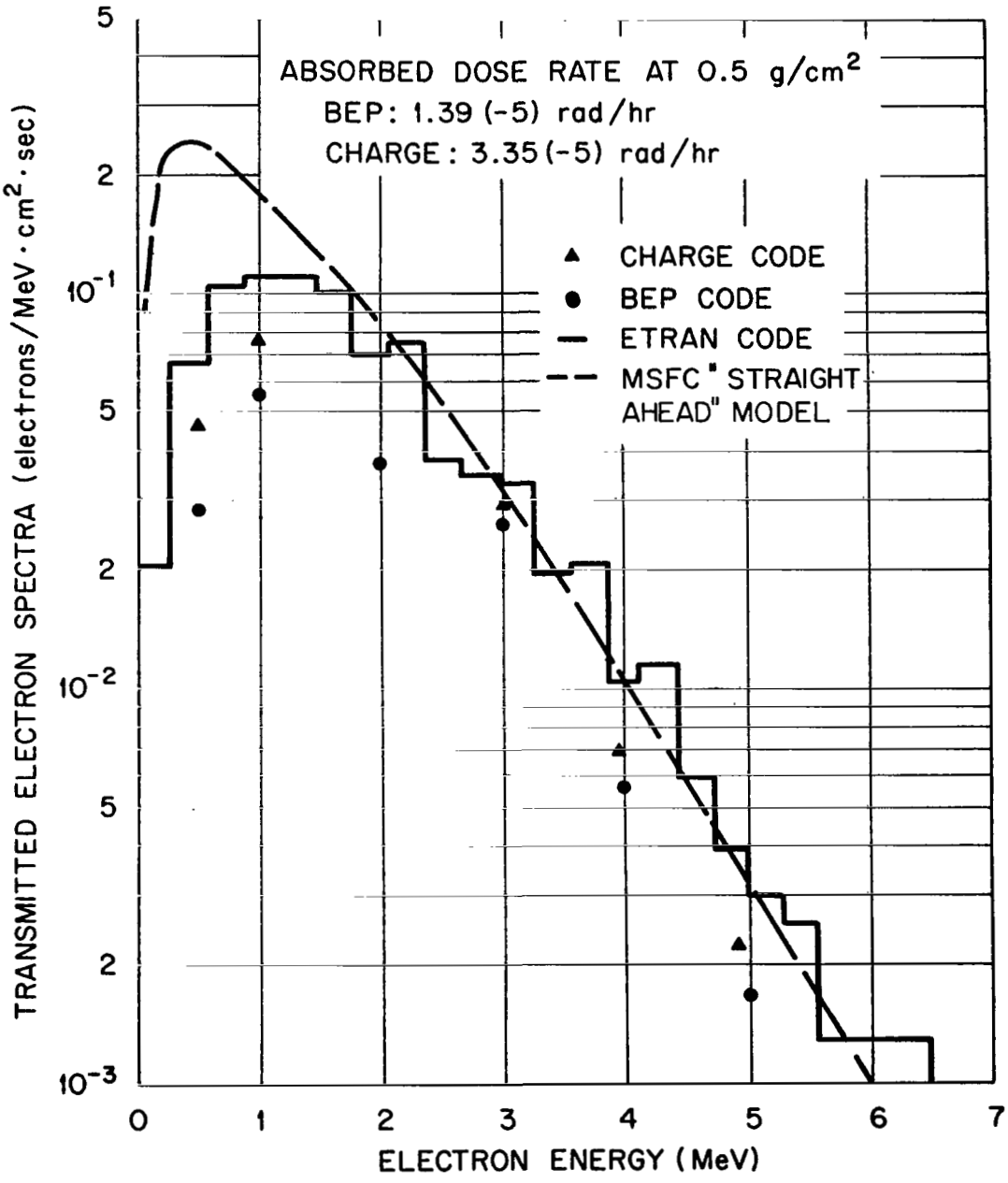

Figure 14. Transmitted electron spectra behind a semi-infinite slab of aluminum of thickness 0.5 g/cm^2.

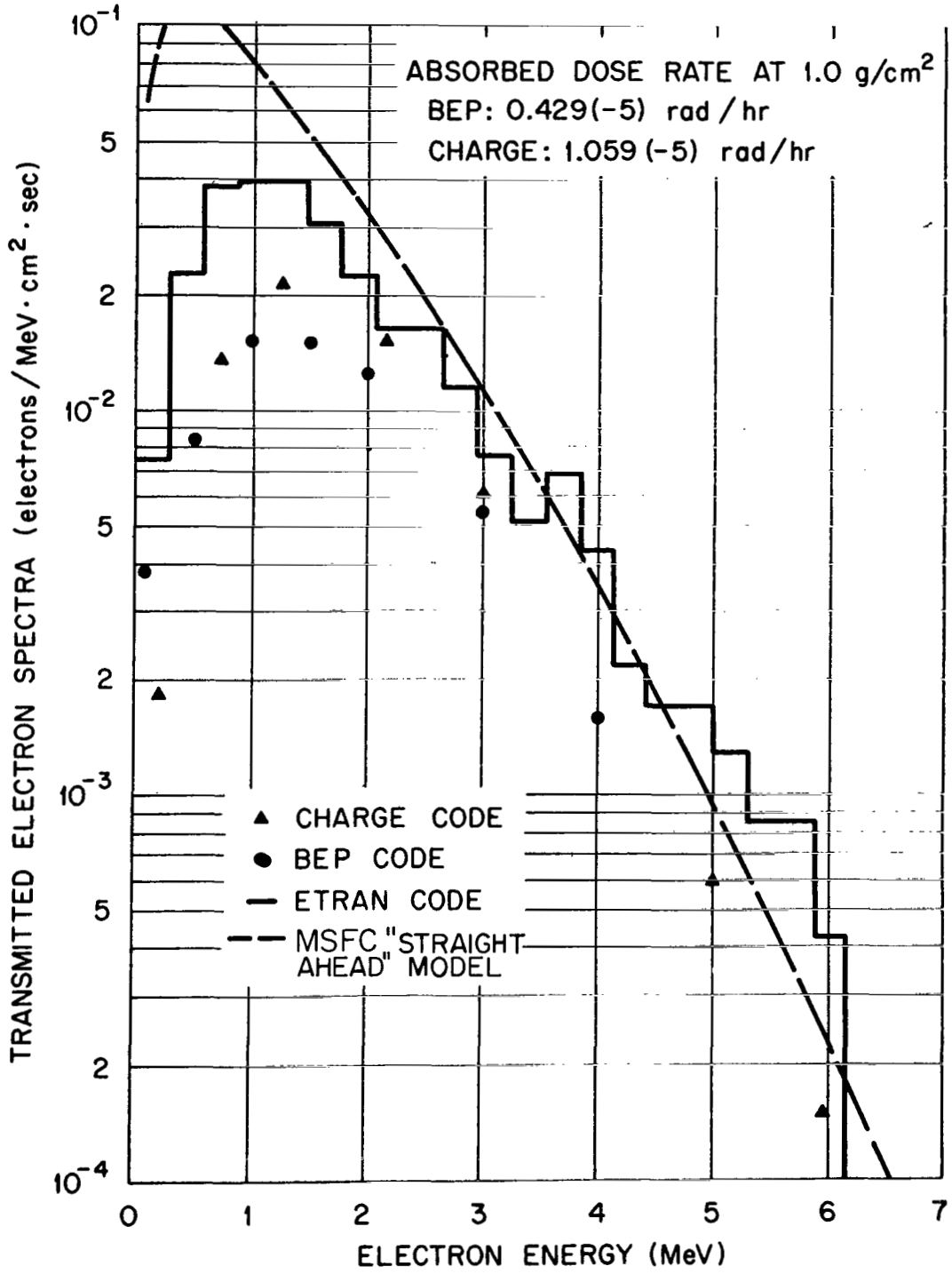

Figure 15. Transmitted electron spectra behind a semi-infinite slab of aluminum of thickness 1.0 g/cm^2.

the receiver does have effectively infinite backing and because the program is relatively easy to use. Where an electron spectrum at an internal point in a shield is needed, the straight-ahead approximation can be used to obtain a conservative estimate of the differential flux. For first-order calculations an estimate of bremsstrahlung dose can be obtained by using equation (57) where the incident electron spectrum falls off exponentially. Where an accurate calculation is needed, equation (49) with a half-space isotropic attenuation kernel should be used. More work needs to be done here in determining the actual source angular distribution.

National Aeronautics and Space Administration
George C. Marshall Space Flight Center
Marshall Space Flight Center, Alabama 35812 December 10, 1970
124-09-21-8023

APPENDIX A

ELECTRON ENERGY CURRENT TRANSMISSION AND REFLECTION COEFFICIENTS FOR AN ALUMINUM PLANE SHIELD

TABLE A-1. ENERGY REFLECTION COEFFICIENT (Energy = 0.5 MeV)

Incident Angle (deg) / Shield Thickness (Z/RO)	0	30	45	60	75	89.9
0.1	0.0120	0.0263	0.0686	0.1802	0.3593	0.7318
0.2	0.0373	0.0659	0.1159	0.2239	0.3894	0.7415
0.3	0.0502	0.0785	0.1248	0.2298	0.3924	0.7425
0.4	0.0511	0.0793	0.1255	0.2302	0.3926	0.7425
0.5	0.0511	0.0793	0.1255	0.2302	0.3926	0.7425
0.6	0.0511	0.0793	0.1255	0.2302	0.3926	0.7425
0.7	0.0511	0.0793	0.1255	0.2302	0.3926	0.7425
0.8	0.0511	0.0793	0.1255	0.2302	0.3926	0.7425
0.9	0.0511	0.0793	0.1255	0.2302	0.3926	0.7425
1.0	0.0511	0.0793	0.1255	0.2302	0.3926	0.7425

TABLE A-2. ENERGY TRANSMISSION COEFFICIENT (Energy = 0.5 MeV)

Incident Angle (deg) / Shield Thickness (Z/RO)	0	30	45	60	75	89.9
0.1	0.9097	0.8772	0.7917	0.6326	0.4407	0.1653
0.2	0.7444	0.6667	0.5586	0.4174	0.2746	0.1061
0.3	0.5379	0.4692	0.3666	0.2620	0.1655	0.0605
0.4	0.3509	0.2861	0.2134	0.1405	0.0825	0.0297
0.5	0.1937	0.1487	0.1005	0.0623	0.0335	0.0107
0.6	0.0814	0.0585	0.0349	0.0197	0.0099	0.0031
0.7	0.0257	0.0156	0.0081	0.0041	0.0016	0.0007
0.8	0.0040	0.0018	0.0007	0.0002	0.0000	0.0000
0.9	0.0001	0.0002	0.0001	0.0000	0.0000	0.0000
1.0	0.0000	0.0000	0.0000	0.0000	0.0000	0.0000

TABLE A-3. ENERGY TRANSMISSION COEFFICIENT (Energy = 1.0 MeV)

Incident Angle (deg) / Shield Thickness (Z/RO)	0	30	45	60	75	89.9
0.1	0.9063	0.8700	0.7868	0.6355	0.4310	0.1532
0.2	0.7508	0.6637	0.5551	0.4142	0.2680	0.0957
0.3	0.5497	0.4564	0.3686	0.2581	0.1574	0.0553
0.4	0.3603	0.2867	0.2202	0.1415	0.0794	0.0266
0.5	0.2035	0.1510	0.1093	0.0630	0.0325	0.0099
0.6	0.0896	0.0603	0.0403	0.0235	0.0095	0.0028
0.7	0.0298	0.0165	0.0107	0.0049	0.0017	0.0006
0.8	0.0051	0.0023	0.0015	0.0005	0.0000	0.0000
0.9	0.0005	0.0001	0.0000	0.0000	0.0000	0.0000
1.0	0.0000	0.0000	0.0000	0.0000	0.0000	0.0000

TABLE A-4. ENERGY REFLECTION COEFFICIENT (Energy = 1.0 MeV)

Incident Angle (deg) / Shield Thickness (Z/RO)	0	30	45	60	75	89.9
0.1	0.0083	0.0214	0.0630	0.1603	0.3403	0.7376
0.2	0.0285	0.0570	0.1051	0.1997	0.3667	0.7459
0.3	0.0395	0.0681	0.1131	0.2051	0.3700	0.7471
0.4	0.0406	0.0689	0.1135	0.2053	0.3701	0.7471
0.5	0.0406	0.0689	0.1135	0.2053	0.3701	0.7471
0.6	0.0406	0.0689	0.1135	0.2053	0.3701	0.7471
0.7	0.0406	0.0689	0.1135	0.2053	0.3701	0.7471
0.8	0.0406	0.0689	0.1135	0.2053	0.3701	0.7471
0.9	0.0406	0.0689	0.1135	0.2053	0.3701	0.7471
1.0	0.0406	0.0689	0.1135	0.2053	0.3701	0.7471

TABLE A-5. ENERGY TRANSMISSION COEFFICIENT (Energy = 2.0 MeV)

Incident Angle (deg) Shield Thickness (Z/RO)	0	30	45	60	75	89.9
0.1	0.9064	0.8745	0.7997	0.6442	0.4264	0.1398
0.2	0.7654	0.6821	0.5656	0.4121	0.2571	0.0864
0.3	0.5840	0.4827	0.3794	0.2553	0.1529	0.0492
0.4	0.4007	0.3109	0.2316	0.1427	0.0785	0.0246
0.5	0.2342	0.1719	0.1194	0.0644	0.0326	0.0092
0.6	0.1126	0.0740	0.0458	0.0231	0.0099	0.0027
0.7	0.0385	0.0232	0.0129	0.0052	0.0017	0.0005
0.8	0.0071	0.0043	0.0021	0.0004	0.0001	0.0000
0.9	0.0007	0.0003	0.0000	0.0000	0.0000	0.0000
1.0	0.0000	0.0000	0.0000	0.0000	0.0000	0.0000

TABLE A-6. ENERGY REFLECTION COEFFICIENT (Energy = 2.0 MeV)

Incident Angle (deg) Shield Thickness (Z/RO)	0	30	45	60	75	89.9
0.1	0.0040	0.0130	0.0422	0.1252	0.3081	0.7409
0.2	0.0140	0.0375	0.0784	0.1607	0.3310	0.7471
0.3	0.0201	0.0446	0.0839	0.1648	0.3336	0.7477
0.4	0.0211	0.0454	0.0842	0.1650	0.3336	0.7477
0.5	0.0211	0.0454	0.0842	0.1650	0.3336	0.7477
0.6	0.0211	0.0454	0.0842	0.1650	0.3336	0.7477
0.7	0.0211	0.0454	0.0842	0.1650	0.3336	0.7477
0.8	0.0211	0.0454	0.0842	0.1650	0.3336	0.7477
0.9	0.0211	0.0454	0.0842	0.1650	0.3336	0.7477
1.0	0.0211	0.0454	0.0842	0.1650	0.3336	0.7477

TABLE A-7. ENERGY TRANSMISSION COEFFICIENT (Energy = 3.0 MeV)

Shield Thickness (Z/RO)	Incident Angle (deg) 0	30	45	60	75	89.9
0.1	0.9048	0.8798	0.8132	0.6643	0.4260	0.1300
0.2	0.7784	0.6992	0.5814	0.4197	0.2492	0.0778
0.3	0.6140	0.5092	0.3955	0.2591	0.1471	0.0444
0.4	0.4296	0.3354	0.2420	0.1451	0.0745	0.0223
0.5	0.2594	0.1943	0.1288	0.0687	0.0301	0.0095
0.6	0.1317	0.0859	0.0534	0.0247	0.0094	0.0026
0.7	0.0490	0.0289	0.0158	0.0060	0.0018	0.0004
0.8	0.0111	0.0053	0.0021	0.0007	0.0001	0.0000
0.9	0.0008	0.0003	0.0002	0.0000	0.0000	0.0000
1.0	0.0000	0.0000	0.0000	0.0000	0.0000	0.0000

TABLE A-8. ENERGY REFLECTION COEFFICIENT (Energy = 3.0 MeV)

Shield Thickness (Z/RO)	Incident Angle (deg) 0	30	45	60	75	89.9
0.1	0.0023	0.0068	0.0288	0.0963	0.2791	0.7424
0.2	0.0077	0.0259	0.0587	0.1293	0.2998	0.7478
0.3	0.0116	0.0313	0.0642	0.1332	0.3018	0.7482
0.4	0.0125	0.0319	0.0644	0.1334	0.3018	0.7482
0.5	0.0125	0.0319	0.0644	0.1334	0.3018	0.7482
0.6	0.0125	0.0319	0.0644	0.1334	0.3018	0.7482
0.7	0.0125	0.0319	0.0644	0.1334	0.3018	0.7482
0.8	0.0125	0.0319	0.0644	0.1334	0.3018	0.7482
0.9	0.0125	0.0319	0.0644	0.1334	0.3018	0.7482
1.0	0.0125	0.0319	0.0644	0.1334	0.3018	0.7482

TABLE A-9. ENERGY TRANSMISSION COEFFICIENT (Energy = 4.0 MeV)

Incident Angle (deg) / Shield Thickness (Z/RO)	0	30	45	60	75	89.9
0.1	0.9035	0.8804	0.8169	0.6694	0.4275	0.1228
0.2	0.7800	0.7064	0.5904	0.4254	0.2482	0.0727
0.3	0.6232	0.5219	0.4020	0.2630	0.1459	0.0412
0.4	0.4473	0.3476	0.2460	0.1470	0.0747	0.0214
0.5	0.2837	0.2081	0.1342	0.0719	0.0318	0.0093
0.6	0.1437	0.1021	0.0598	0.0274	0.0100	0.0028
0.7	0.0607	0.0366	0.0189	0.0065	0.0020	0.0004
0.8	0.0163	0.0086	0.0035	0.0008	0.0003	0.0000
0.9	0.0021	0.0008	0.0003	0.0000	0.0000	0.0000
1.0	0.0000	0.0000	0.0000	0.0000	0.0000	0.0000

TABLE A-10. ENERGY REFLECTION COEFFICIENT (Energy = 4.0 MeV)

Incident Angle (deg) / Shield Thickness (Z/RO)	0	30	45	60	75	89.9
0.1	0.0016	0.0053	0.0227	0.0829	0.2616	0.7462
0.2	0.0051	0.0193	0.0466	0.1136	0.2816	0.7509
0.3	0.0081	0.0245	0.0508	0.1169	0.2832	0.7512
0.4	0.0086	0.0248	0.0511	0.1172	0.2832	0.7512
0.5	0.0086	0.0248	0.0511	0.1172	0.2832	0.7512
0.6	0.0086	0.0248	0.0511	0.1172	0.2832	0.7512
0.7	0.0086	0.0248	0.0511	0.1172	0.2832	0.7512
0.8	0.0086	0.0248	0.0511	0.1172	0.2832	0.7512
0.9	0.0086	0.0248	0.0511	0.1172	0.2832	0.7512
1.0	0.0086	0.0248	0.0511	0.1172	0.2832	0.7512

TABLE A-11. ENERGY TRANSMISSION COEFFICIENT (Energy= 5.0 MeV)

Incident Angle (deg)						
Shield Thickness (Z/RO)	0	30	45	60	75	89.9
0.1	0.9033	0.8821	0.8281	0.6852	0.4280	0.1149
0.2	0.7866	0.7187	0.6026	0.4341	0.2427	0.0655
0.3	0.6428	0.5376	0.4133	0.2688	0.1408	0.0369
0.4	0.4751	0.3643	0.2558	0.1508	0.0719	0.0192
0.5	0.3054	0.2189	0.1412	0.0721	0.0318	0.0082
0.6	0.1686	0.1119	0.0647	0.0274	0.0106	0.0025
0.7	0.0711	0.0441	0.0205	0.0075	0.0026	0.0005
0.8	0.0186	0.0099	0.0044	0.0010	0.0004	0.0000
0.9	0.0027	0.0010	0.0005	0.0001	0.0000	0.0000
1.0	0.0000	0.0000	0.0000	0.0000	0.0000	0.0000

TABLE A-12. ENERGY REFLECTION COEFFICIENT (Energy = 5.0 MeV)

Incident Angle (deg)						
Shield Thickness (Z/RO)	0	30	45	60	75	89.9
0.1	0.0013	0.0033	0.0158	0.0660	0.2400	0.7474
0.2	0.0042	0.0131	0.0349	0.0933	0.2584	0.7515
0.3	0.0065	0.0162	0.0385	0.0965	0.2599	0.7517
0.4	0.0072	0.0162	0.0386	0.0966	0.2599	0.7517
0.5	0.0072	0.0162	0.0386	0.0966	0.2599	0.7517
0.6	0.0072	0.0162	0.0386	0.0966	0.2599	0.7517
0.7	0.0072	0.0162	0.0386	0.0966	0.2599	0.7517
0.8	0.0072	0.0162	0.0386	0.0966	0.2599	0.7517
0.9	0.0072	0.0162	0.0386	0.0966	0.2599	0.7517
1.0	0.0072	0.0162	0.0386	0.0966	0.2599	0.7517

TABLE A-13. ENERGY TRANSMISSION COEFFICIENT (Energy = 6.0 MeV)

Shield Thickness (Z/RO)	Incident Angle (deg) 0	30	45	60	75	89.9
0.1	0.9027	0.8810	0.8327	0.6911	0.4279	0.1106
0.2	0.7891	0.7247	0.6078	0.4354	0.2386	0.0626
0.3	0.6488	0.5458	0.4181	0.2666	0.1397	0.0340
0.4	0.4877	0.3778	0.2619	0.1521	0.0726	0.0169
0.5	0.3212	0.2348	0.1456	0.0745	0.0316	0.0069
0.6	0.1856	0.1240	0.0678	0.0287	0.0106	0.0021
0.7	0.0808	0.0503	0.0232	0.0081	0.0022	0.0004
0.8	0.0229	0.0130	0.0048	0.0013	0.0003	0.0000
0.9	0.0037	0.0015	0.0006	0.0002	0.0000	0.0000
1.0	0.0000	0.0000	0.0000	0.0000	0.0000	0.0000

TABLE A-14. ENERGY REFLECTION COEFFICIENT (Energy = 6.0 MeV)

Shield Thickness (Z/RO)	Incident Angle (deg) 0	30	45	60	75	89.9
0.1	0.0013	0.0026	0.0120	0.0577	0.2252	0.7483
0.2	0.0031	0.0089	0.0294	0.0818	0.2418	0.7520
0.3	0.0053	0.0118	0.0327	0.0850	0.2432	0.7522
0.4	0.0060	0.0118	0.0328	0.0851	0.2432	0.7522
0.5	0.0060	0.0118	0.0328	0.0851	0.2432	0.7522
0.6	0.0060	0.0118	0.0328	0.0851	0.2432	0.7522
0.7	0.0060	0.0118	0.0328	0.0851	0.2432	0.7522
0.8	0.0060	0.0118	0.0328	0.0851	0.2432	0.7522
0.9	0.0060	0.0118	0.0328	0.0851	0.2432	0.7522
1.0	0.0060	0.0118	0.0328	0.0851	0.2432	0.7522

TABLE A-15. ENERGY TRANSMISSION COEFFICIENT (Energy = 10.0 MeV)

Incident Angle (deg)						
Shield Thickness (Z/RO)	0	30	45	60	75	89.9
0.1	0.8991	0.8773	0.8374	0.7114	0.4448	0.0821
0.2	0.7844	0.7329	0.6349	0.4516	0.2479	0.0440
0.3	0.6587	0.5714	0.4464	0.2787	0.1336	0.0226
0.4	0.5200	0.4050	0.2936	0.1626	0.0656	0.0108
0.5	0.3716	0.2634	0.1756	0.0824	0.0268	0.0040
0.6	0.2271	0.1500	0.0902	0.0354	0.0089	0.0012
0.7	0.1144	0.0679	0.0350	0.0115	0.0020	0.0002
0.8	0.0413	0.0210	0.0098	0.0022	0.0003	0.0000
0.9	0.0087	0.0039	0.0013	0.0001	0.0000	0.0000
1.0	0.0007	0.0001	0.0000	0.0000	0.0000	0.0000

TABLE A-16. ENERGY REFLECTION COEFFICIENT (Energy = 10.0 MeV)

Incident Angle (deg)						
Shield Thickness (Z/RO)	0	30	45	60	75	89.9
0.1	0.0005	0.0029	0.0076	0.0382	0.1779	0.7905
0.2	0.0014	0.0049	0.0162	0.0543	0.1920	0.7928
0.3	0.0022	0.0065	0.0181	0.0566	0.1927	0.7929
0.4	0.0024	0.0067	0.0181	0.0567	0.1927	0.7929
0.5	0.0024	0.0067	0.0181	0.0567	0.1927	0.7929
0.6	0.0024	0.0067	0.0181	0.0567	0.1927	0.7929
0.7	0.0024	0.0067	0.0181	0.0567	0.1927	0.7929
0.8	0.0024	0.0067	0.0181	0.0567	0.1927	0.7929
0.9	0.0024	0.0067	0.0181	0.0567	0.1927	0.7929
1.0	0.0024	0.0067	0.0181	0.0567	0.1927	0.7929

APPENDIX B

ELECTRON NUMBER CURRENT TRANSMISSION AND REFLECTION COEFFICIENTS FOR AN ALUMINUM PLANE SHIELD

TABLE B-1. NUMBER TRANSMISSION COEFFICIENT (Energy = 0.5 MeV)

Incident Angle (deg)						
Shield Thickness (Z/RO)	0	30	45	60	75	89.9
0.1	0.9912	0.9696	0.9120	0.7657	0.5600	0.2162
0.2	0.9188	0.8540	0.7557	0.5963	0.4227	0.1675
0.3	0.7732	0.6960	0.5853	0.4437	0.3003	0.1125
0.4	0.6004	0.5072	0.4060	0.2837	0.1793	0.0667
0.5	0.4012	0.3236	0.2323	0.1527	0.0856	0.0290
0.6	0.2032	0.1512	0.0953	0.0563	0.0313	0.0095
0.7	0.0752	0.0500	0.0270	0.0150	0.0060	0.0032
0.8	0.0164	0.0064	0.0006	0.0013	0.0003	0.0000
0.9	0.0008	0.0012	0.0023	0.0000	0.0000	0.0000
1.0	0.0000	0.0004	0.0000	0.0000	0.0000	0.0000

TABLE B-2. NUMBER REFLECTION COEFFICIENT (Energy = 0.5 MeV)

Incident Angle (deg)						
Shield Thickness (Z/RO)	0	30	45	60	75	89.9
0.1	0.0176	0.0396	0.0970	0.2493	0.4510	0.7892
0.2	0.0656	0.1180	0.1910	0.3417	0.5160	0.8115
0.3	0.0984	0.1516	0.2177	0.3597	0.5267	0.8142
0.4	0.1020	0.1548	0.2203	0.3610	0.5267	0.8145
0.5	0.1020	0.1548	0.2203	0.3610	0.5267	0.8145
0.6	0.1020	0.1548	0.2203	0.3610	0.5267	0.8145
0.7	0.1020	0.1548	0.2203	0.3610	0.5267	0.8145
0.8	0.1020	0.1548	0.2203	0.3610	0.5267	0.8145
0.9	0.1020	0.1548	0.2203	0.3610	0.5267	0.8145
1.0	0.1020	0.1548	0.2203	0.3610	0.5267	0.8145

TABLE B-3. NUMBER TRANSMISSION COEFFICIENT (Energy = 1.0 MeV)

Incident Angle (deg)						
Shield Thickness (Z/RO)	0	30	45	60	75	89.9
0.1	0.9976	0.9797	0.9208	0.7900	0.5780	0.2114
0.2	0.9436	0.8767	0.7763	0.6286	0.4411	0.1626
0.3	0.8176	0.7183	0.6189	0.4699	0.3104	0.1116
0.4	0.6432	0.5433	0.4429	0.3107	0.1884	0.0651
0.5	0.4428	0.3560	0.2709	0.1678	0.0937	0.0284
0.6	0.2424	0.1763	0.1237	0.1036	0.0333	0.0092
0.7	0.1028	0.0613	0.0397	0.0207	0.0077	0.0028
0.8	0.0232	0.0123	0.0000	0.0028	0.0002	0.0005
0.9	0.0024	0.0010	0.0077	0.0000	0.0000	0.0000
1.0	0.0000	0.0000	0.0000	0.0000	0.0000	0.0000

TABLE B-4. NUMBER REFLECTION COEFFICIENT (Energy = 1.0 MeV)

Incident Angle (deg)						
Shield Thickness (Z/RO)	0	30	45	60	75	89.9
0.1	0.0132	0.0350	0.0962	0.2347	0.4533	0.8157
0.2	0.0556	0.1103	0.1874	0.3253	0.5187	0.8371
0.3	0.0868	0.1440	0.2143	0.3433	0.5302	0.8418
0.4	0.0920	0.1470	0.2160	0.3446	0.5309	0.8418
0.5	0.0920	0.1470	0.2160	0.3446	0.5309	0.8418
0.6	0.0920	0.1470	0.2160	0.3446	0.5309	0.8418
0.7	0.0920	0.1470	0.2160	0.3446	0.5309	0.8418
0.8	0.0920	0.1470	0.2160	0.3610	0.5309	0.8418
0.9	0.0920	0.1470	0.2160	0.3446	0.5309	0.8418
1.0	0.0920	0.1470	0.2160	0.3446	0.5309	0.8418

TABLE B-5. NUMBER TRANSMISSION COEFFICIENT (Energy = 2.0 MeV)

Shield Thickness (Z/RO)	Incident Angle (deg) 0	30	45	60	75	89.9
0.1	1.0120	0.9980	0.9531	0.8295	0.5969	0.2060
0.2	0.9772	0.9213	0.8188	0.6650	0.4518	0.1577
0.3	0.8892	0.7833	0.6683	0.4962	0.3251	0.1077
0.4	0.7388	0.6110	0.4946	0.3415	0.2027	0.0671
0.5	0.5380	0.4253	0.3154	0.1880	0.1022	0.0308
0.6	0.3284	0.2323	0.1491	0.0845	0.0384	0.0177
0.7	0.1460	0.0926	0.5286	0.0235	0.0082	0.0027
0.8	0.0348	0.0223	0.0005	0.0032	0.0011	0.0001
0.9	0.0044	0.0020	0.0108	0.0002	0.0002	0.0000
1.0	0.0008	0.0000	0.0000	0.0000	0.0000	0.0000

TABLE B-6. NUMBER REFLECTION COEFFICIENT (Energy = 2.0 MeV)

Shield Thickness (Z/RO)	Incident Angle (deg) 0	30	45	60	75	89.9
0.1	0.0100	0.0246	0.0714	0.2015	0.4420	0.8261
0.2	0.0332	0.0813	0.1577	0.2935	0.5064	0.8435
0.3	0.0548	0.1067	0.1789	0.3102	0.5160	0.8463
0.4	0.0592	0.1107	0.1806	0.3115	0.5162	0.8464
0.5	0.0592	0.1107	0.1806	0.3115	0.5162	0.8464
0.6	0.0592	0.1107	0.1806	0.3115	0.5162	0.8464
0.7	0.0592	0.1107	0.1806	0.3115	0.5162	0.8464
0.8	0.0592	0.1107	0.1806	0.3446	0.5162	0.8464
0.9	0.0592	0.1107	0.1806	0.3115	0.5162	0.8464
1.0	0.0592	0.1107	0.1806	0.3115	0.5162	0.8464

TABLE B-7. NUMBER TRANSMISSION COEFFICIENT (Energy = 3.0 MeV)

Incident Angle (deg)						
Shield Thickness (Z/RO)	0	30	45	60	75	89.9
0.1	1.0180	1.0100	0.9797	0.8790	0.6282	0.2020
0.2	1.0010	0.9530	0.8548	0.6977	0.4653	0.1537
0.3	0.9424	0.8387	0.7123	0.5285	0.3336	0.1071
0.4	0.7968	0.6727	0.5343	0.3620	0.2098	0.0638
0.5	0.6092	0.4960	0.3563	0.2122	0.1053	0.0334
0.6	0.3900	0.2803	0.1843	0.0972	0.0406	0.0121
0.7	0.1928	0.1237	0.0731	0.0300	0.0111	0.0025
0.8	0.0588	0.0300	0.0014	0.0050	0.0013	0.0002
0.9	0.0060	0.0023	0.0134	0.0000	0.0000	0.0000
1.0	0.0004	0.0000	0.0000	0.0000	0.0000	0.0000

TABLE B-8. NUMBER REFLECTION COEFFICIENT (Energy = 3.0 MeV)

Incident Angle (deg)						
Shield Thickness (Z/RO)	0	30	45	60	75	89.9
0.1	0.0052	0.0163	0.0565	0.1705	0.4389	0.8470
0.2	0.0180	0.0650	0.1351	0.2650	0.5058	0.8643
0.3	0.0312	0.0860	0.1577	0.2830	0.5151	0.8665
0.4	0.0352	0.0890	0.1586	0.2840	0.5153	0.8665
0.5	0.0352	0.0890	0.1586	0.2840	0.5153	0.8665
0.6	0.0352	0.0890	0.1586	0.2840	0.5153	0.8665
0.7	0.0352	0.0890	0.1586	0.2840	0.5153	0.8665
0.8	0.0352	0.0890	0.1586	0.3115	0.5153	0.8665
0.9	0.0352	0.0890	0.1586	0.2840	0.5153	0.8665
1.0	0.0352	0.0890	0.1586	0.2840	0.5153	0.8665

TABLE B-9. NUMBER TRANSMISSION COEFFICIENT (Energy = 4.0 MeV)

Incident Angle (deg)						
Shield Thickness (Z/RO)	0	30	45	60	75	89.9
0.1	1.0260	1.0200	0.9906	0.8925	0.6453	0.1980
0.2	1.0150	0.9723	0.8777	0.7195	0.4756	0.1473
0.3	0.9624	0.8703	0.7383	0.5542	0.3456	0.1027
0.4	0.8441	0.7103	0.5543	0.3787	0.2169	0.0652
0.5	0.6769	0.5350	0.3789	0.2325	0.1144	0.0354
0.6	0.4605	0.3380	0.2149	0.1140	0.0440	0.0137
0.7	0.2449	0.1570	0.0880	0.0355	0.0117	0.0024
0.8	0.0899	0.0510	0.0025	0.0060	0.0024	0.0007
0.9	0.0159	0.0066	0.0231	0.0005	0.0004	0.0000
1.0	0.0007	0.0003	0.0000	0.0000	0.0000	0.0000

TABLE B-10. NUMBER REFLECTION COEFFICIENT (Energy = 4.0 MeV)

Incident Angle (deg)						
Shield Thickness (Z/RO)	0	30	45	60	75	89.9
0.1	0.0050	0.0146	0.0491	0.1590	0.4364	0.8667
0.2	0.0146	0.0523	0.1151	0.2540	0.5040	0.8833
0.3	0.0267	0.0746	0.1329	0.2710	0.5122	0.8853
0.4	0.0299	0.0760	0.1343	0.2722	0.5124	0.8854
0.5	0.0301	0.0760	0.1343	0.2722	0.5124	0.8854
0.6	0.0301	0.0760	0.1343	0.2722	0.5124	0.8854
0.7	0.0301	0.0760	0.1343	0.2722	0.5124	0.8854
0.8	0.0301	0.0760	0.1343	0.2840	0.5124	0.8854
0.9	0.0301	0.0760	0.1343	0.2722	0.5124	0.8854
1.0	0.0301	0.0760	0.1343	0.2722	0.5124	0.8854

TABLE B-11. NUMBER TRANSMISSION COEFFICIENT (Energy = 5.0 MeV)

Shield Thickness (Z/RO)	Incident Angle (deg) 0	30	45	60	75	89.9
0.1	1.0330	1.0220	1.0020	0.9237	0.6593	0.1924
0.2	1.0240	0.9880	0.9057	0.7515	0.4862	0.1409
0.3	0.9852	0.9007	0.7660	0.5795	0.3444	0.0940
0.4	0.8856	0.7497	0.5897	0.4075	0.2156	0.0618
0.5	0.7132	0.5657	0.4097	0.2400	0.1167	0.0328
0.6	0.5032	0.3703	0.2394	0.1145	0.0488	0.0127
0.7	0.2812	0.1917	0.0985	0.0400	0.0146	0.0032
0.8	0.1024	0.0593	0.0045	0.0085	0.0024	0.0002
0.9	0.0216	0.0100	0.0277	0.0010	0.0004	0.0000
1.0	0.0004	0.0000	0.0000	0.0000	0.0000	0.0000

TABLE B-12. NUMBER REFLECTION COEFFICIENT (Energy = 5.0 MeV)

Shield Thickness (Z/RO)	Incident Angle (deg) 0	30	45	60	75	89.9
0.1	0.0048	0.0090	0.0397	0.1390	0.4271	0.8885
0.2	0.0108	0.0370	0.0985	0.2287	0.4929	0.9038
0.3	0.0192	0.0506	0.1151	0.2450	0.5018	0.9055
0.4	0.0228	0.0520	0.1157	0.2457	0.5018	0.9055
0.5	0.0228	0.0520	0.1157	0.2457	0.5018	0.9055
0.6	0.0228	0.0520	0.1157	0.2457	0.5018	0.9055
0.7	0.0228	0.0520	0.1157	0.2457	0.5018	0.9055
0.8	0.0228	0.0520	0.1157	0.2722	0.5018	0.9055
0.9	0.0228	0.0520	0.1157	0.2457	0.5018	0.9055
1.0	0.0228	0.0520	0.1157	0.2457	0.5018	0.9055

TABLE B-13. NUMBER TRANSMISSION COEFFICIENT (Energy = 6.0 MeV)

Shield Thickness (Z/RO)	Incident Angle (deg) 0	30	45	60	75	89.9
0.1	1.0320	1.0250	1.0150	0.9380	0.6778	0.1894
0.2	1.0340	1.0010	0.9200	0.7605	0.4929	0.1380
0.3	0.9896	0.9120	0.7828	0.5875	0.3542	0.0918
0.4	0.9092	0.7830	0.6129	0.4212	0.2236	0.0567
0.5	0.7548	0.6033	0.4263	0.2525	0.1242	0.0284
0.6	0.5576	0.4090	0.2520	0.1235	0.0515	0.0110
0.7	0.3232	0.2180	0.1169	0.0465	0.0140	0.0031
0.8	0.1268	0.0773	0.0051	0.0102	0.0026	0.0002
0.9	0.0272	0.0140	0.0314	0.0015	0.0002	0.0000
1.0	0.0000	0.0000	0.0000	0.0000	0.0000	0.0000

TABLE B-14. NUMBER REFLECTION COEFFICIENT (Energy = 6.0 MeV)

Shield Thickness (Z/RO)	Incident Angle (deg) 0	30	45	60	75	89.9
0.1	0.0056	0.0103	0.0302	0.1310	0.4240	0.8995
0.2	0.0096	0.0283	0.0842	0.2130	0.4878	0.9155
0.3	0.0176	0.0397	0.1000	0.2292	0.4962	0.9165
0.4	0.0204	0.0416	0.1003	0.2300	0.4962	0.9167
0.5	0.0204	0.0416	0.1003	0.2300	0.4962	0.9167
0.6	0.0204	0.0416	0.1003	0.2300	0.4962	0.9167
0.7	0.0204	0.0416	0.1003	0.2300	0.4962	0.9167
0.8	0.0204	0.0416	0.1003	0.2300	0.4962	0.9167
0.9	0.0204	0.0416	0.1003	0.2300	0.4962	0.9167
1.0	0.0204	0.0416	0.1003	0.2300	0.4962	0.9167

TABLE B-15. NUMBER TRANSMISSION COEFFICIENT (Energy = 10.0 MeV)

Incident Angle (deg)						
Shield Thickness (Z/RO)	0	30	45	60	75	89.9
0.1	1.0480	1.0420	1.0280	0.9830	0.7378	0.1540
0.2	1.0460	1.0320	0.9834	0.8282	0.5553	0.1103
0.3	1.0210	0.9787	0.8583	0.6532	0.3804	0.0737
0.4	0.9648	0.8473	0.7143	0.4712	0.2338	0.0437
0.5	0.8700	0.6930	0.5314	0.3040	0.1178	0.0200
0.6	0.6820	0.4987	0.3457	0.1600	0.0488	0.0072
0.7	0.4480	0.2987	0.1746	0.0665	0.0135	0.0018
0.8	0.2240	0.1307	0.0697	0.0180	0.0026	0.0002
0.9	0.0688	0.0313	0.0122	0.0025	0.0006	0.0000
1.0	0.0084	0.0020	0.0011	0.0000	0.0000	0.0000

TABLE B-16. NUMBER REFLECTION COEFFICIENT (Energy = 10.0 MeV)

Incident Angle (deg)						
Shield Thickness (Z/RO)	0	30	45	60	75	89.9
0.1	0.0052	0.0106	0.0254	0.1012	0.3831	0.9437
0.2	0.0088	0.0166	0.0565	0.1665	0.4449	0.9556
0.3	0.0120	0.0233	0.0680	0.1810	0.4502	0.9558
0.4	0.0132	0.0246	0.0682	0.1817	0.4502	0.9558
0.5	0.0132	0.0250	0.0682	0.1817	0.4502	0.9558
0.6	0.0132	0.0250	0.0682	0.1817	0.4502	0.9558
0.7	0.0132	0.0250	0.0682	0.1817	0.4502	0.9558
0.8	0.0132	0.0250	0.0682	0.1817	0.4502	0.9558
0.9	0.0132	0.0250	0.0682	0.1817	0.4502	0.9558
1.0	0.0132	0.0250	0.0682	0.1817	0.4502	0.9558

APPENDIX C

ELECTRON ENERGY DEPOSITION COEFFICIENTS IN MeV/g FOR AN ALUMINUM SEMI-INFINITE PLANE SHIELD

TABLE C-1. ENERGY DEPOSITION COEFFICIENT (Energy = 0.5 MeV)

INCIDENT ANGLE (DEGREES)	0	30	45	60	75	89.9
SHIELD THICKNESS (Z/RO)						
0.01	2.0000	2.5400	3.3100	5.2900	8.7800	6.3700
0.03	2.3400	3.0100	4.1000	6.0900	5.7700	2.0700
0.05	2.7100	3.5300	4.6400	5.5100	4.3400	1.7000
0.07	2.9300	3.6300	4.9800	4.9500	3.8800	1.4800
0.09	3.1000	3.8500	4.7100	4.5000	3.5300	1.2900
0.11	3.4500	3.9400	4.6400	4.3100	3.2400	1.2200
0.13	3.5800	4.1300	4.3200	3.9300	2.9000	1.1200
0.15	3.8000	4.2700	4.2900	3.7900	2.8500	1.0900
0.17	4.0500	4.0400	4.1100	3.5700	2.6200	1.0600
0.19	4.1000	4.4000	4.0300	3.4100	2.6200	1.0000
0.21	4.2900	4.2000	3.8000	3.1300	2.3500	0.9900
0.23	4.1300	4.2100	3.7500	3.0200	2.3000	0.9100
0.25	4.2100	3.9100	3.7800	3.0600	2.1800	0.8900
0.27	4.0600	4.0100	3.5300	2.9200	1.9800	0.7900
0.29	3.9200	3.8000	3.3700	2.6200	1.9000	0.7500
0.31	3.9400	3.7900	3.2200	2.5700	1.8400	0.7000
0.33	3.6800	3.6600	3.0400	2.4500	1.6800	0.6100
0.35	3.7400	3.2900	3.0900	2.2900	1.6200	0.6400
0.37	3.4800	3.3600	3.0000	2.1900	1.3900	0.5300
0.39	3.4200	3.2800	2.8800	2.0700	1.3300	0.5000
0.41	3.4300	3.0600	2.5000	1.9100	1.1700	0.4800
0.43	3.1800	2.7300	2.2400	1.6700	1.0900	0.3800
0.45	3.0800	2.6100	2.0900	1.4300	0.8800	0.3500
0.47	3.0300	2.4100	2.0200	1.3100	0.8300	0.3000
0.49	2.9900	2.3200	1.8600	1.1700	0.6900	0.2500
0.51	2.7100	2.1700	1.6700	1.0900	0.6800	0.2100
0.53	2.2700	1.9800	1.3500	0.8400	0.5900	0.1900
0.55	2.2100	1.7200	1.2700	0.8400	0.4000	0.1600
0.57	1.9100	1.4700	1.1200	0.7400	0.4100	0.1200
0.59	1.7200	1.1600	0.8900	0.5600	0.3200	0.1000
0.61	1.5400	1.1000	0.7700	0.4300	0.2700	0.0800
0.63	1.2200	0.9500	0.5600	0.3600	0.1800	0.0600
0.65	0.9700	0.7600	0.4400	0.2800	0.1300	0.0600
0.67	0.7400	0.6400	0.3800	0.2100	0.0900	0.0400
0.69	0.6900	0.5800	0.3000	0.1500	0.0700	0.0300
0.71	0.5500	0.4100	0.2200	0.1400	0.0500	0.0300
0.73	0.5000	0.2800	0.1800	0.1200	0.0500	0.0300
0.75	0.4300	0.2500	0.1200	0.0800	0.0200	0.0100
0.77	0.3500	0.1500	0.0700	0.0400	0.0100	0.0100
0.79	0.2400	0.1500	0.0400	0.0300	0.0100	0.0000
0.81	0.1800	0.1000	0.0200	0.0200	0.0000	0.0000
0.83	0.0900	0.0300	0.0100	0.0000	0.0000	0.0000
0.85	0.0600	0.0200	0.0100	0.0000	0.0000	0.0000
0.87	0.0200	0.0100	0.0100	0.0000	0.0000	0.0000
0.89	0.0100	0.0100	0.0100	0.0000	0.0000	0.0000
0.91	0.0000	0.0100	0.0100	0.0000	0.0000	0.0000
0.93	0.0000	0.0000	0.0100	0.0000	0.0000	0.0000

TABLE C-2. ENERGY DEPOSITION COEFFICIENT (Energy = 1.0 MeV)

INCIDENT ANGLE (DEGREES)	0	30	45	60	75	89.9
SHIELD THICKNESS (Z/RO)						
0.01	1.7700	2.0900	2.9000	4.4700	7.9500	5.4100
0.03	1.8700	2.3900	3.3000	5.2000	5.2500	1.8600
0.05	2.1800	2.7900	3.7800	4.8700	4.0300	1.4600
0.07	2.3100	3.0200	3.9700	4.3400	3.3600	1.2200
0.09	2.4200	3.2600	3.8800	3.9100	3.0600	1.0600
0.11	2.6500	3.3400	3.7500	3.7000	2.7200	0.9800
0.13	2.9600	3.4100	3.6000	3.3900	2.5000	0.9000
0.15	3.1100	3.5100	3.7000	3.1300	2.3500	0.8600
0.17	3.1600	3.6600	3.5300	3.0000	2.2100	0.8000
0.19	3.4300	3.5900	3.4300	2.8100	2.1000	0.7900
0.21	3.3700	3.4000	3.1900	2.7400	2.0600	0.7200
0.23	3.3000	3.3800	3.0500	2.5800	1.7400	0.6500
0.25	3.3500	3.2000	2.8800	2.5500	1.7400	0.6200
0.27	3.3400	3.1600	2.7700	2.3400	1.6600	0.5600
0.29	3.2900	3.1100	2.7500	2.2000	1.5300	0.5500
0.31	3.1700	2.9500	2.6100	2.0200	1.4400	0.5500
0.33	3.1600	2.8000	2.4100	1.9700	1.2500	0.5100
0.35	3.0200	2.7100	2.3800	1.7800	1.2100	0.4600
0.37	3.0200	2.7300	2.2100	1.7200	1.0900	0.4600
0.39	2.9400	2.6800	2.1000	1.6300	1.0500	0.4100
0.41	2.7400	2.4500	2.0900	1.4900	0.9100	0.3300
0.43	2.6800	2.3500	1.9300	1.3600	0.8400	0.2800
0.45	2.4900	2.0800	1.7400	1.2400	0.7100	0.2600
0.47	2.4600	2.0200	1.6300	1.0800	0.6000	0.2100
0.49	2.3400	1.8700	1.5800	0.9800	0.5800	0.1800
0.51	2.1100	1.7500	1.3800	0.9200	0.5100	0.1400
0.53	1.9800	1.5300	1.1500	0.7700	0.4500	0.1300
0.55	1.7100	1.4500	1.1400	0.6600	0.3900	0.1000
0.57	1.5600	1.2700	1.0100	0.5600	0.3000	0.0900
0.59	1.4000	1.1400	0.8100	0.4800	0.2200	0.0800
0.61	1.1300	0.9000	0.6200	0.3700	0.1800	0.0500
0.63	1.1100	0.7600	0.5300	0.2900	0.1700	0.0400
0.65	1.0400	0.7000	0.4700	0.2500	0.1000	0.0300
0.67	0.7500	0.5500	0.3500	0.1900	0.0800	0.0200
0.69	0.7400	0.4600	0.2900	0.1600	0.0600	0.0200
0.71	0.5700	0.3500	0.2300	0.1400	0.0500	0.0200
0.73	0.4900	0.2800	0.1700	0.0900	0.0300	0.0200
0.75	0.3600	0.2000	0.1500	0.0600	0.0400	0.0000
0.77	0.2900	0.1500	0.1100	0.0400	0.0200	0.0000
0.79	0.2000	0.1000	0.0700	0.0200	0.0100	0.0000
0.81	0.1500	0.0900	0.0400	0.0200	0.0000	0.0000
0.83	0.0900	0.0500	0.0300	0.0100	0.0000	0.0000
0.85	0.0600	0.0300	0.0300	0.0100	0.0000	0.0000
0.87	0.0400	0.0200	0.0100	0.0000	0.0000	0.0000
0.89	0.0200	0.0100	0.0000	0.0000	0.0000	0.0000
0.91	0.0100	0.0000	0.0000	0.0000	0.0000	0.0000
0.93	0.0100	0.0000	0.0000	0.0000	0.0000	0.0000
0.95	0.0100	0.0000	0.0000	0.0000	0.0000	0.0000

TABLE C-3. ENERGY DEPOSITION COEFFICIENT (Energy = 2.0 MeV)

INCIDENT ANGLE (DEGREES)	0	30	45	60	75	89.9
SHIELD THICKNESS (Z/RO)						
0.01	1.5300	1.9100	2.6100	4.1600	7.8700	5.2400
0.03	1.6300	2.1200	3.0100	4.9200	5.3300	1.7600
0.05	1.8300	2.3500	3.3400	4.7900	4.1100	1.3200
0.07	1.9200	2.5600	3.4500	4.2100	3.4600	1.0800
0.09	2.0300	2.7100	3.4600	3.8200	2.9600	0.9800
0.11	2.2700	2.9100	3.5100	3.5400	2.6900	0.8400
0.13	2.4200	2.9000	3.3000	3.3000	2.4200	0.7800
0.15	2.4400	3.1000	3.1900	3.1800	2.1700	0.7600
0.17	2.5900	3.1700	3.2400	2.9100	2.0000	0.7000
0.19	2.7100	3.0900	3.0900	2.6500	1.9300	0.6400
0.21	2.8500	3.1600	2.8300	2.5800	1.7700	0.6100
0.23	2.9200	2.9900	2.8400	2.4100	1.5900	0.6200
0.25	2.8600	2.9400	2.7400	2.1800	1.4700	0.5500
0.27	2.9000	2.8800	2.7600	2.0100	1.4100	0.5000
0.29	2.8800	2.7400	2.5200	2.0000	1.3300	0.4600
0.31	2.6800	2.7100	2.4300	1.8700	1.2400	0.4000
0.33	2.8100	2.6700	2.3100	1.7300	1.1500	0.4000
0.35	2.8100	2.5500	2.1900	1.6100	1.0900	0.3600
0.37	2.6400	2.4200	2.1100	1.5400	0.9800	0.3300
0.39	2.8100	2.4300	2.0700	1.4000	0.9500	0.2900
0.41	2.6600	2.3500	1.8900	1.3400	0.8000	0.2800
0.43	2.6300	2.1900	1.7600	1.2500	0.7500	0.2600
0.45	2.4300	2.0200	1.6400	1.1900	0.7000	0.2300
0.47	2.4400	1.8900	1.5100	1.0700	0.5700	0.2000
0.49	2.3600	1.8000	1.4600	0.8700	0.5100	0.1500
0.51	2.0900	1.6600	1.3200	0.8100	0.4400	0.1300
0.53	1.9200	1.5400	1.1600	0.6900	0.3700	0.1200
0.55	1.7100	1.3700	1.0500	0.5800	0.3200	0.0800
0.57	1.6400	1.2900	0.8900	0.4900	0.2800	0.0700
0.59	1.5400	1.1500	0.7800	0.4100	0.2300	0.0700
0.61	1.2900	0.9500	0.6600	0.3800	0.1700	0.0500
0.63	1.2000	0.8500	0.5600	0.3200	0.1500	0.0300
0.65	0.9900	0.7400	0.5100	0.2600	0.1000	0.0300
0.67	0.8700	0.6800	0.4000	0.1800	0.0700	0.0200
0.69	0.7700	0.5000	0.3200	0.1400	0.0500	0.0100
0.71	0.6000	0.4100	0.2500	0.1200	0.0300	0.0100
0.73	0.5300	0.3400	0.1900	0.0900	0.0200	0.0100
0.75	0.4700	0.2600	0.1400	0.0700	0.0100	0.0100
0.77	0.3900	0.2200	0.1200	0.0600	0.0100	0.0100
0.79	0.2700	0.1900	0.0700	0.0300	0.0000	0.0000
0.81	0.1700	0.1100	0.0600	0.0100	0.0000	0.0000
0.83	0.1200	0.0800	0.0300	0.0100	0.0000	0.0000
0.85	0.0700	0.0400	0.0200	0.0000	0.0000	0.0000
0.87	0.0500	0.0200	0.0200	0.0000	0.0000	0.0000
0.89	0.0500	0.0200	0.0100	0.0000	0.0000	0.0000
0.91	0.0100	0.0100	0.0000	0.0000	0.0000	0.0000
0.93	0.0100	0.0100	0.0000	0.0000	0.0000	0.0000
0.95	0.0100	0.0000	0.0000	0.0000	0.0000	0.0000

TABLE C-4. ENERGY DEPOSITION COEFFICIENT (Energy = 3.0 MeV)

INCIDENT ANGLE (DEGREES)	0	30	45	60	75	89.9
SHIELD THICKNESS (Z/RO)						
0.01	1.4300	1.8300	2.4600	3.9200	8.1500	5.4500
0.03	1.5200	1.9300	2.8500	4.7900	5.7400	1.8200
0.05	1.7300	2.1800	3.0900	4.8000	4.5200	1.3200
0.07	1.7700	2.2800	3.3400	4.4400	3.6500	1.1100
0.09	1.8800	2.4900	3.3300	3.9400	3.2600	0.9300
0.11	2.0100	2.6500	3.3100	3.7900	2.7700	0.8000
0.13	2.0500	2.6500	3.3400	3.5600	2.4400	0.7800
0.15	2.2100	2.7500	3.2800	3.2000	2.2600	0.7000
0.17	2.3700	2.8000	3.2200	2.9500	2.0900	0.6700
0.19	2.4500	2.8600	3.0000	2.7400	1.8500	0.6100
0.21	2.5800	2.9000	2.9400	2.5100	1.7000	0.5800
0.23	2.6600	2.9700	2.7000	2.3500	1.5900	0.5100
0.25	2.5800	2.9300	2.6800	2.2500	1.4600	0.4800
0.27	2.6700	2.7800	2.5800	2.0900	1.3800	0.4200
0.29	2.7500	2.8000	2.5400	1.9600	1.3000	0.4200
0.31	2.8200	2.5600	2.3600	1.8800	1.1800	0.3900
0.33	2.7900	2.7200	2.3000	1.7400	1.1400	0.3600
0.35	2.8000	2.5800	2.2500	1.6200	1.0100	0.3000
0.37	2.8600	2.5200	2.1500	1.4600	0.9400	0.2700
0.39	2.8800	2.4600	1.9900	1.4000	0.8700	0.2500
0.41	2.7200	2.2700	1.8200	1.3000	0.8000	0.2300
0.43	2.5500	2.1500	1.8000	1.1900	0.7300	0.1900
0.45	2.4400	2.0600	1.6400	1.1200	0.6100	0.1800
0.47	2.3100	2.0100	1.5800	1.0200	0.5500	0.1700
0.49	2.2500	1.8800	1.4500	0.8800	0.4800	0.1500
0.51	2.0900	1.7500	1.3100	0.8000	0.4100	0.1400
0.53	1.9200	1.6800	1.2800	0.7200	0.3300	0.1200
0.55	1.7900	1.5800	1.1200	0.6500	0.2700	0.1000
0.57	1.7000	1.3400	0.9300	0.5100	0.2200	0.0800
0.59	1.6100	1.2300	0.8400	0.4700	0.1900	0.0700
0.61	1.4400	1.0700	0.7000	0.3900	0.1600	0.0600
0.63	1.3100	0.9500	0.5800	0.2900	0.1200	0.0300
0.65	1.1600	0.8400	0.5200	0.2800	0.1100	0.0300
0.67	1.0500	0.6800	0.4600	0.2000	0.0800	0.0200
0.69	0.8900	0.5500	0.3800	0.1700	0.0700	0.0200
0.71	0.8000	0.4900	0.3300	0.1200	0.0400	0.0100
0.73	0.5800	0.4200	0.2700	0.0900	0.0400	0.0100
0.75	0.5100	0.3300	0.1600	0.0800	0.0200	0.0000
0.77	0.4300	0.2500	0.1100	0.0600	0.0200	0.0000
0.79	0.3800	0.1900	0.0800	0.0300	0.0100	0.0000
0.81	0.2500	0.1500	0.0600	0.0200	0.0000	0.0000
0.83	0.2000	0.0900	0.0400	0.0200	0.0000	0.0000
0.85	0.1200	0.0700	0.0200	0.0100	0.0000	0.0000
0.87	0.0900	0.0300	0.0100	0.0100	0.0000	0.0000
0.89	0.0500	0.0100	0.0100	0.0000	0.0000	0.0000
0.91	0.0200	0.0100	0.0100	0.0000	0.0000	0.0000
0.93	0.0100	0.0100	0.0000	0.0000	0.0000	0.0000
0.95	0.0200	0.0100	0.0000	0.0000	0.0000	0.0000
0.97	0.0100	0.0000	0.0000	0.0000	0.0000	0.0000

TABLE C-5. ENERGY DEPOSITION COEFFICIENT (Energy = 4.0 MeV)

INCIDENT ANGLE (DEGREES)	0	30	45	60	75	89.9
SHIELD THICKNESS (Z/RO)						
0.01	1.4400	1.7800	2.4000	3.9500	8.3100	5.5600
0.03	1.5500	1.9000	2.7100	4.6900	5.9900	1.8300
0.05	1.6100	2.0500	3.0100	4.8300	4.6700	1.3000
0.07	1.7100	2.1900	3.2100	4.4800	3.8700	1.0800
0.09	1.7900	2.3700	3.3300	4.0800	3.3800	0.9000
0.11	1.8800	2.4300	3.3300	3.7200	2.8200	0.8000
0.13	1.9900	2.6100	3.3200	3.4400	2.5600	0.7100
0.15	2.0400	2.6500	3.2600	3.2200	2.3300	0.7000
0.17	2.1700	2.7600	3.1900	2.8900	2.0400	0.6500
0.19	2.2700	2.8500	3.1300	2.7400	1.8500	0.5700
0.21	2.3600	2.7800	2.9800	2.6000	1.7000	0.4900
0.23	2.4300	2.8800	2.8200	2.4100	1.5500	0.4700
0.25	2.5200	2.8200	2.7900	2.2500	1.3700	0.4500
0.27	2.6100	2.7900	2.6300	2.1000	1.3800	0.4300
0.29	2.6700	2.7100	2.5500	1.9700	1.2600	0.4000
0.31	2.6600	2.6000	2.4600	1.8700	1.1700	0.3500
0.33	2.7100	2.6600	2.3100	1.7900	1.0800	0.3100
0.35	2.6500	2.5900	2.2000	1.6300	1.0000	0.2800
0.37	2.6700	2.5000	2.1400	1.6100	0.9500	0.2600
0.39	2.6300	2.4200	2.0000	1.4400	0.8900	0.2300
0.41	2.5700	2.2800	1.8800	1.2600	0.7700	0.2300
0.43	2.5400	2.0800	1.7500	1.1600	0.6700	0.1800
0.45	2.4700	2.0400	1.6500	1.1400	0.6300	0.1800
0.47	2.3400	1.9900	1.5000	0.9900	0.5200	0.1600
0.49	2.2900	1.9200	1.4600	0.9200	0.4700	0.1500
0.51	2.2100	1.8500	1.2900	0.7900	0.4200	0.1300
0.53	2.1000	1.6800	1.1800	0.7400	0.3400	0.1100
0.55	1.9700	1.4900	1.0800	0.6800	0.3200	0.0900
0.57	1.8400	1.3700	0.9700	0.5800	0.2800	0.0800
0.59	1.6900	1.2900	0.8700	0.4700	0.2000	0.0500
0.61	1.5800	1.1600	0.7600	0.4400	0.1700	0.0500
0.63	1.4500	1.0400	0.6300	0.3600	0.1300	0.0400
0.65	1.3000	0.9400	0.5700	0.3200	0.1100	0.0300
0.67	1.1600	0.8200	0.5100	0.2200	0.0900	0.0300
0.69	1.0000	0.7300	0.4000	0.1700	0.0700	0.0200
0.71	0.8600	0.5500	0.3200	0.1400	0.0400	0.0100
0.73	0.7500	0.5000	0.2500	0.1000	0.0300	0.0100
0.75	0.6400	0.4000	0.2300	0.0700	0.0200	0.0000
0.77	0.5400	0.3000	0.1600	0.0500	0.0100	0.0000
0.79	0.4300	0.2200	0.1200	0.0500	0.0100	0.0000
0.81	0.3500	0.2000	0.0800	0.0200	0.0100	0.0000
0.83	0.2600	0.1400	0.0700	0.0100	0.0100	0.0000
0.85	0.1900	0.1100	0.0400	0.0100	0.0000	0.0000
0.87	0.1300	0.0700	0.0300	0.0000	0.0000	0.0000
0.89	0.0900	0.0400	0.0200	0.0000	0.0000	0.0000
0.91	0.0600	0.0300	0.0100	0.0000	0.0000	0.0000
0.93	0.0400	0.0200	0.0100	0.0000	0.0000	0.0000
0.95	0.0300	0.0100	0.0000	0.0000	0.0000	0.0000
0.97	0.0100	0.0000	0.0000	0.0000	0.0000	0.0000
0.99	0.0100	0.0000	0.0000	0.0000	0.0000	0.0000

TABLE C-6. ENERGY DEPOSITION COEFFICIENT (Energy = 5.0 MeV)

INCIDENT ANGLE (DEGREES)	0	30	45	60	75	89.9
SHIELD THICKNESS (Z/RO)						
0.01	1.4300	1.7200	2.3100	3.7800	8.4400	5.8500
0.03	1.5100	1.8800	2.6100	4.5300	6.5000	1.8900
0.05	1.6300	1.9400	2.8600	4.7700	5.0000	1.2900
0.07	1.6200	2.1100	3.1000	4.5300	4.1700	1.0700
0.09	1.6700	2.2400	3.1900	4.2100	3.5400	0.9200
0.11	1.7800	2.3300	3.2000	3.8900	2.9700	0.7900
0.13	1.7500	2.4100	3.2900	3.5400	2.6200	0.7200
0.15	1.8400	2.6000	3.3900	3.3200	2.3800	0.6800
0.17	2.0200	2.7900	3.2900	3.0800	2.1200	0.5800
0.19	2.1100	2.7900	3.1700	2.8500	1.9200	0.5800
0.21	2.1600	2.6700	2.9900	2.6300	1.7300	0.4800
0.23	2.2400	2.7400	2.8300	2.5000	1.5700	0.4500
0.25	2.3200	2.7500	2.8700	2.3500	1.4400	0.4200
0.27	2.5300	2.7700	2.6800	2.2000	1.2900	0.3800
0.29	2.4300	2.7100	2.5800	2.0600	1.2200	0.3400
0.31	2.4800	2.6600	2.5000	1.9200	1.1300	0.2900
0.33	2.6000	2.6700	2.3900	1.8100	1.1100	0.2800
0.35	2.6200	2.5300	2.3000	1.7300	1.0100	0.2600
0.37	2.6900	2.5900	2.1900	1.7000	0.8900	0.2200
0.39	2.7100	2.6500	2.1000	1.5300	0.7900	0.2400
0.41	2.6200	2.2700	1.9300	1.4100	0.7500	0.2000
0.43	2.4900	2.2700	1.8300	1.2400	0.6400	0.1800
0.45	2.5800	2.1500	1.7100	1.2000	0.5600	0.1500
0.47	2.4200	2.0100	1.5400	1.0500	0.5200	0.1300
0.49	2.4100	1.9300	1.4400	0.9100	0.4600	0.1400
0.51	2.2900	1.8600	1.3800	0.8300	0.4100	0.1100
0.53	2.1800	1.7100	1.1900	0.7400	0.3600	0.0900
0.55	2.0800	1.6000	1.0600	0.6600	0.2900	0.0800
0.57	1.9400	1.4500	1.0100	0.5600	0.2500	0.0700
0.59	1.8300	1.3200	0.9600	0.4800	0.2100	0.0600
0.61	1.6400	1.2700	0.8500	0.4100	0.1900	0.0500
0.63	1.5300	1.0800	0.7000	0.3200	0.1400	0.0300
0.65	1.4100	0.9700	0.6000	0.1200	0.1100	0.0300
0.67	1.2800	0.8600	0.5300	0.0800	0.0800	0.0200
0.69	1.1400	0.7400	0.4300	0.0700	0.0600	0.0200
0.71	1.0500	0.6800	0.3300	0.0500	0.0600	0.0100
0.73	0.8400	0.5900	0.2600	0.0300	0.0400	0.0100
0.75	0.7200	0.5000	0.2300	0.0200	0.0400	0.0100
0.77	0.6100	0.3900	0.1900	0.0100	0.0200	0.0000
0.79	0.5000	0.2900	0.1600	0.0000	0.0100	0.0000
0.81	0.4000	0.2300	0.1000	0.0000	0.0100	0.0000
0.83	0.2900	0.1900	0.0700	0.0000	0.0100	0.0000
0.85	0.2000	0.1200	0.0400	0.0000	0.0000	0.0000
0.87	0.1600	0.0800	0.0500	0.0000	0.0000	0.0000
0.89	0.1000	0.0600	0.0300	0.0000	0.0000	0.0000
0.91	0.0800	0.0400	0.0100	0.0000	0.0000	0.0000
0.93	0.0500	0.0100	0.0100	0.0000	0.0000	0.0000
0.95	0.0500	0.0100	0.0100	0.0000	0.0000	0.0000
0.97	0.0300	0.0000	0.0000	0.0000	0.0000	0.0000

TABLE C-7. ENERGY DEPOSITION COEFFICIENT (Energy = 6.0 MeV)

INCIDENT ANGLE (DEGREES)	0	30	45	60	75	89.9
SHIELD THICKNESS (Z/RO)						
0.01	1.4200	1.7300	2.3000	3.6900	8.5400	5.9500
0.03	1.4900	1.8900	2.5700	4.4600	6.7900	1.8900
0.05	1.5900	1.9700	2.7400	4.7400	5.2700	1.3700
0.07	1.6100	2.0600	2.9800	4.5500	4.3400	1.1300
0.09	1.6200	2.1200	3.1100	4.3500	3.6500	0.9000
0.11	1.7000	2.2600	3.1800	4.0900	3.0700	0.7900
0.13	1.7100	2.4200	3.2900	3.6700	2.7300	0.7400
0.15	1.8500	2.4600	3.2500	3.4500	2.4300	0.6400
0.17	1.9300	2.6500	3.3400	3.0900	2.2300	0.5800
0.19	2.0500	2.7400	3.1500	2.9300	1.9200	0.5200
0.21	2.1200	2.6900	3.0200	2.6900	1.6300	0.5000
0.23	2.1800	2.6800	2.8600	2.5200	1.5500	0.4600
0.25	2.3100	2.6800	2.9100	2.3700	1.4400	0.3900
0.27	2.3900	2.7500	2.7800	2.2000	1.2800	0.3700
0.29	2.4900	2.6600	2.5400	2.0700	1.2000	0.3600
0.31	2.3500	2.5600	2.4700	1.8600	1.1400	0.3000
0.33	2.5100	2.5900	2.3600	1.7900	1.0700	0.2700
0.35	2.5000	2.6500	2.3200	1.7400	1.0200	0.2500
0.37	2.5300	2.5600	2.2100	1.6200	0.9000	0.2100
0.39	2.6900	2.4400	2.1000	1.5400	0.8400	0.2100
0.41	2.5900	2.2900	1.9500	1.4000	0.7100	0.1800
0.43	2.5300	2.2800	1.8400	1.2600	0.6500	0.1700
0.45	2.3900	2.1300	1.7400	1.1500	0.6000	0.1600
0.47	2.4400	2.0200	1.5800	1.0100	0.5600	0.1300
0.49	2.3400	1.9200	1.4900	0.9000	0.4700	0.1100
0.51	2.2700	1.8100	1.3700	0.8300	0.4200	0.0900
0.53	2.2000	1.7800	1.3000	0.7600	0.3500	0.0700
0.55	2.0400	1.6500	1.1700	0.6900	0.3000	0.0700
0.57	1.9600	1.6500	1.0800	0.5800	0.2400	0.0600
0.59	1.9600	1.4700	1.0000	0.5000	0.2300	0.0400
0.61	1.8000	1.3600	0.8600	0.4300	0.1700	0.0400
0.63	1.6300	1.1100	0.7100	0.3600	0.1600	0.0300
0.65	1.5200	1.0900	0.6400	0.2800	0.1300	0.0300
0.67	1.3800	1.0100	0.5200	0.2400	0.1000	0.0200
0.69	1.2200	0.8700	0.4500	0.2100	0.0700	0.0100
0.71	1.1100	0.7300	0.4100	0.1500	0.0500	0.0100
0.73	0.9400	0.6500	0.3200	0.1300	0.0300	0.0100
0.75	0.8600	0.5200	0.2500	0.0800	0.0300	0.0100
0.77	0.7300	0.4400	0.2100	0.0700	0.0100	0.0000
0.79	0.6400	0.3600	0.1500	0.0600	0.0100	0.0000
0.81	0.4700	0.2800	0.1100	0.0300	0.0100	0.0000
0.83	0.3200	0.2100	0.0600	0.0200	0.0100	0.0000
0.85	0.2600	0.1600	0.0500	0.0100	0.0000	0.0000
0.87	0.1900	0.1000	0.0400	0.0000	0.0000	0.0000
0.89	0.1300	0.0600	0.0200	0.0000	0.0000	0.0000
0.91	0.1000	0.0600	0.0100	0.0000	0.0000	0.0000
0.93	0.0600	0.0400	0.0200	0.0000	0.0000	0.0000
0.95	0.0400	0.0200	0.0200	0.0000	0.0000	0.0000
0.97	0.0300	0.0100	0.0100	0.0000	0.0000	0.0000
0.99	0.0200	0.0000	0.0000	0.0000	0.0000	0.0000

TABLE C-8. ENERGY DEPOSITION COEFFICIENT (Energy = 10.0 MeV)

INCIDENT ANGLE (DEGREES)	0	30	45	60	75	89.9
SHIELD THICKNESS (Z/RO)						
0.01	1.4500	1.6900	2.2100	3.5500	8.6400	5.1000
0.03	1.4800	1.8100	2.3800	4.2400	7.6200	1.7600
0.05	1.5200	1.8300	2.5400	4.4500	5.9000	1.2700
0.07	1.5900	2.0300	2.7200	4.5600	4.6500	1.0200
0.09	1.6700	2.0000	2.9000	4.4900	3.7200	0.8200
0.11	1.6400	2.1000	2.9800	4.1100	3.3100	0.7200
0.13	1.7600	2.2400	3.0500	3.9000	2.9700	0.5900
0.15	1.7700	2.2500	3.0600	3.6500	2.6600	0.5000
0.17	1.7800	2.3200	3.1400	3.4300	2.4100	0.4700
0.19	1.8300	2.3600	3.1000	3.2000	2.2600	0.4100
0.21	1.9600	2.4500	2.9700	2.9500	2.0300	0.3800
0.23	1.9300	2.5000	2.9200	2.7400	1.7900	0.3700
0.25	1.9700	2.5600	2.7900	2.4600	1.6500	0.3300
0.27	2.0700	2.6200	2.7600	2.3100	1.4600	0.2800
0.29	2.0800	2.6100	2.7200	2.1800	1.3000	0.2400
0.31	2.0700	2.6500	2.6100	2.0300	1.2300	0.2300
0.33	2.1500	2.6100	2.4400	1.9000	1.1500	0.2000
0.35	2.1900	2.6300	2.3200	1.7800	1.0500	0.1800
0.37	2.3200	2.4500	2.1500	1.6600	0.9500	0.1700
0.39	2.2700	2.3700	2.0700	1.5600	0.8400	0.1600
0.41	2.3900	2.2400	2.0400	1.4400	0.7200	0.1400
0.43	2.4300	2.2600	1.9200	1.3700	0.6700	0.1100
0.45	2.3400	2.2500	1.8000	1.2500	0.5900	0.1000
0.47	2.3200	2.1600	1.7400	1.0900	0.5200	0.0900
0.49	2.3400	2.0400	1.6500	0.9800	0.4400	0.0800
0.51	2.4500	1.9800	1.5700	0.9200	0.3700	0.0600
0.53	2.3400	1.8600	1.4500	0.7900	0.3200	0.0500
0.55	2.2800	1.7700	1.3200	0.7000	0.2700	0.0400
0.57	2.1800	1.6400	1.2500	0.6300	0.2300	0.0400
0.59	2.0700	1.6000	1.1300	0.5200	0.1800	0.0300
0.61	1.9400	1.4900	1.0700	0.4600	0.1500	0.0200
0.63	1.8900	1.4100	0.9500	0.4500	0.1200	0.0200
0.65	1.7700	1.2600	0.8900	0.3900	0.1000	0.0100
0.67	1.6200	1.1400	0.7600	0.2900	0.0900	0.0100
0.69	1.5100	1.0400	0.6200	0.2700	0.0600	0.0100
0.71	1.3800	0.9400	0.5500	0.2100	0.0400	0.0100
0.73	1.3600	0.8500	0.4400	0.1700	0.0400	0.0100
0.75	1.1700	0.6900	0.3700	0.1500	0.0300	0.0000
0.77	0.9700	0.6100	0.3000	0.1000	0.0100	0.0000
0.79	0.8700	0.5300	0.2800	0.0700	0.0100	0.0000
0.81	0.7000	0.3800	0.2300	0.0600	0.0100	0.0000
0.83	0.6000	0.3300	0.1900	0.0400	0.0100	0.0000
0.85	0.4600	0.2600	0.1100	0.0400	0.0000	0.0000
0.87	0.3900	0.1900	0.0800	0.0200	0.0000	0.0000
0.89	0.3100	0.1700	0.0600	0.0100	0.0000	0.0000
0.91	0.2200	0.1000	0.0400	0.0100	0.0000	0.0000
0.93	0.1500	0.0800	0.0200	0.0100	0.0000	0.0000
0.95	0.1000	0.0500	0.0100	0.0000	0.0000	0.0000
0.97	0.0700	0.0400	0.0100	0.0000	0.0000	0.0000
0.99	0.0400	0.0200	0.0100	0.0000	0.0000	0.0000

APPENDIX D

ELECTRON PATHLENGTH IN ALUMINUM AS A FUNCTION OF ELECTRON INITIAL ENERGY [3]

TABLE D-1. ELECTRON PATHLENGTH IN ALUMINUM AS A FUNCTION OF ELECTRON INITIAL ENERGY

Electron Energy (MeV)	Mean Pathlength (g/cm^2)
0.01	3.519×10^{-4}
0.02	1.165×10^{-3}
0.04	3.883×10^{-3}
0.06	7.822×10^{-3}
0.08	1.279×10^{-2}
0.10	1.864×10^{-2}
0.20	5.772×10^{-2}
0.40	1.640×10^{-1}
0.60	2.871×10^{-1}
0.80	4.168×10^{-1}
1.00	5.493×10^{-1}
1.5	8.825×10^{-1}
2.0	1.212
3.0	1.855
4.0	2.476
5.0	3.076
6.0	3.658
7.0	4.225
8.0	4.777
9.0	5.315
10.0	5.841

APPENDIX E

ELECTRON ENERGY DEPOSITION COEFFICIENTS IN MeV/g FOR A HALF-SPACE ISOTROPIC INCIDENT BEAM ON AN ALUMINUM SEMI-INFINITE PLANE SHIELD

TABLE E-1. ISOTROPIC ENERGY DEPOSITION COEFFICIENTS

INCIDENT ENERGY (MEV) / SHIELD THICKNESS (PATHLENGTHS)	0.5	1	2	3	4	5	6	10
0.01	2.1151	1.8368	1.7236	1.6841	1.6854	1.6567	1.6544	1.6312
0.03	2.1534	1.8064	1.6960	1.6611	1.6489	1.6532	1.6632	1.6672
0.05	2.1410	1.8097	1.6726	1.6446	1.6250	1.6103	1.6148	1.5833
0.07	2.1133	1.7640	1.6082	1.5869	1.5760	1.5748	1.5672	1.5539
0.09	2.0430	1.7225	1.5557	1.5369	1.5399	1.5243	1.5183	1.4976
0.11	2.0211	1.6798	1.5509	1.5095	1.4711	1.4655	1.4784	1.4461
0.13	1.9466	1.6354	1.4837	1.4652	1.4504	1.4222	1.4441	1.4339
0.15	1.9542	1.6299	1.4668	1.4269	1.4095	1.4239	1.4048	1.3889
0.17	1.8698	1.6071	1.4481	1.3941	1.3647	1.4010	1.3927	1.3641
0.19	1.8955	1.5688	1.3903	1.3376	1.3439	1.3500	1.3462	1.3308
0.21	1.8020	1.4981	1.3542	1.3056	1.2928	1.2745	1.2730	1.2887
0.23	1.7683	1.4325	1.3028	1.2633	1.2581	1.2417	1.2348	1.2470
0.25	1.7289	1.3848	1.2463	1.2305	1.2192	1.2259	1.2228	1.2001
0.27	1.6721	1.3360	1.2194	1.1777	1.1836	1.1872	1.1895	1.1788
0.29	1.5832	1.2990	1.1611	1.1592	1.1420	1.1408	1.1312	1.1466
0.31	1.5492	1.2267	1.1246	1.0882	1.0969	1.1041	1.0742	1.1131
0.33	1.4704	1.1598	1.0784	1.0836	1.0733	1.0840	1.0593	1.0729
0.35	1.4057	1.1130	1.0288	1.0351	1.0233	1.0376	1.0530	1.0419
0.37	1.3632	1.0787	0.9762	0.9943	0.9980	1.0230	1.0058	0.9807
0.39	1.3164	1.0411	0.9634	0.9547	0.9441	0.9951	0.9695	0.9377
0.41	1.2083	0.9720	0.9042	0.8826	0.8772	0.8997	0.8995	0.8993
0.43	1.0848	0.9154	0.8502	0.8378	0.8133	0.8541	0.8616	0.8775
0.45	1.0022	0.8213	0.7911	0.7828	0.7864	0.8159	0.8054	0.8375
0.47	0.9460	0.7718	0.7340	0.7465	0.7295	0.7477	0.7539	0.7936
0.49	0.8853	0.7262	0.6849	0.6884	0.7006	0.7036	0.7048	0.7483
0.51	0.8172	0.6611	0.6227	0.6307	0.6477	0.6679	0.6594	0.7232
0.53	0.6949	0.5740	0.5590	0.5941	0.5930	0.6039	0.6301	0.6660
0.55	0.6307	0.5320	0.4953	0.5413	0.5393	0.5531	0.5762	0.6225
0.57	0.5520	0.4653	0.4477	0.4602	0.4884	0.5051	0.5445	0.5799
0.59	0.4438	0.3992	0.3967	0.4224	0.4393	0.4635	0.4996	0.5380
0.61	0.3936	0.3134	0.3259	0.3630	0.3962	0.4243	0.4466	0.4999
0.63	0.3161	0.2719	0.2944	0.3106	0.3449	0.3597	0.3759	0.4677
0.65	0.2496	0.2428	0.2522	0.2786	0.3101	0.3019	0.3479	0.4252
0.67	0.2034	0.1845	0.2131	0.2323	0.2666	0.2647	0.3081	0.3730
0.69	0.1744	0.1590	0.1669	0.1921	0.2253	0.2258	0.2663	0.3315
0.71	0.1310	0.1248	0.1335	0.1653	0.1776	0.1981	0.2282	0.2943
0.73	0.1031	0.0965	0.1087	0.1343	0.1513	0.1628	0.1937	0.2624
0.75	0.0812	0.0740	0.0853	0.1014	0.1254	0.1394	0.1572	0.2189
0.77	0.0519	0.0548	0.0722	0.0778	0.0947	0.1110	0.1320	0.1822
0.79	0.0417	0.0355	0.0518	0.0592	0.0730	0.0859	0.1078	0.1603
0.81	0.0274	0.0271	0.0323	0.0429	0.0581	0.0651	0.0800	0.1236
0.83	0.0098	0.0162	0.0219	0.0295	0.0429	0.0503	0.0555	0.1045
0.85	0.0069	0.0119	0.0115	0.0192	0.0307	0.0316	0.0424	0.0770
0.87	0.0036	0.0060	0.0077	0.0109	0.0199	0.0253	0.0283	0.0578
0.89	0.0031	0.0023	0.0064	0.0050	0.0125	0.0170	0.0172	0.0475
0.91	0.0026	0.0004	0.0018	0.0036	0.0083	0.0107	0.0145	0.0300
0.93	0.0012	0.0004	0.0018	0.0018	0.0060	0.0050	0.0110	0.0221
0.95	0.0000	0.0004	0.0000	0.0023	0.0028	0.0050	0.0072	0.0131
0.97	0.0000	0.0000	0.0000	0.0000	0.0004	0.0014	0.0041	0.0102
0.99	0.0000	0.0000	0.0000	0.0000	0.0004	0.0000	0.0009	0.0060

APPENDIX F

CURVE FIT COEFFICIENTS FOR THE ENERGY DEPOSITION COEFFICIENT DERIVED FROM THE ENERGY CURRENT TRANSMISSION AND REFLECTION COEFFICIENTS IN APPENDIX A

The Functional Form is

$$\rho(E,\theta,X) = \frac{E}{r_0(E)} \left[-A\ (B+2CX+3DX^2)\ e^{(BX+CX^2+DX^3)} \right]$$

TABLE F-1. CURVE FIT COEFFICIENTS FOR θ = 0 DEGREES

Energy (MeV)	A	B	C	D
0.5	0.9509	-0.4708	-3.367	-4.402
1.0	0.9607	-0.6268	-2.461	-5.194
2.0	0.9816	-0.7250	-1.750	-5.155
3.0	0.9905	-0.8595	-6.267	-5.949
4.0	0.9983	-0.9428	-0.04876	-5.481
5.0	0.9960	-0.8681	-0.7710	-5.032
6.0	1.002	-0.9431	-0.1163	-4.899
10.0	1.018	-0.9930	-0.1161	-3.619

TABLE F-2. CURVE FIT COEFFICIENTS FOR θ = 30 DEGREES

Energy (MeV)	A	B	C	D
0.5	0.9221	-0.5920	-4.826	-3.032
1.0	0.9321	-0.8037	-3.967	-3.974
2.0	0.9568	-0.8430	-3.758	-3.197
3.0	0.9732	-0.8541	-3.569	-2.493
4.0	0.9827	-0.8646	-3.449	-1.911
5.0	0.9902	-0.9242	-2.768	-2.717
6.0	0.9961	-0.9671	-2.469	-2.644
10.0	1.004	-1.071	-1.701	-2.734

TABLE F-3. CURVE FIT COEFFICIENTS FOR θ = 45 DEGREES

Energy (MeV)	A	B	C	D
0.5	0.8749	-1.223	-4.509	-4.063
1.0	0.8875	-1.397	-4.289	-3.091
2.0	0.9174	-1.469	-4.269	-2.403
3.0	0.9386	-1.376	-4.751	-1.249
4.0	0.9529	-1.363	-4.899	-0.6228
5.0	0.9675	-1.238	-5.468	0.4328
6.0	0.9756	-1.202	-5.661	1.013
10.0	0.9932	-1.240	-4.610	0.4896

TABLE F-4. CURVE FIT COEFFICIENTS FOR θ = 60 DEGREES

Energy (MeV)	A	B	C	D
0.5	0.7699	-2.550	-1.075	-8.375
1.0	0.7949	-2.702	-1.640	-6.482
2.0	0.8352	-2.825	-2.486	-4.788
3.0	0.8671	-2.864	-3.010	-3.446
4.0	0.8833	-2.957	-2.652	-3.599
5.0	0.9042	-2.880	-3.238	-2.702
6.0	0.9162	-2.795	-4.216	-0.9783
10.0	0.9758	-2.354	-6.701	5.590

TABLE F-5. CURVE FIT COEFFICIENTS FOR θ = 75 DEGREES

Energy (MeV)	A	B	C	D
0.5	1.134	-1.979	1.021	0.2902
1.0	1.029	-2.498	1.448	0.2135
2.0	0.6664	-4.500	0.7975	-8.555
3.0	0.9320	-3.877	2.976	-0.3942
4.0	0.7167	-6.022	6.305	-13.60
5.0	0.7401	-6.827	9.069	-15.77
6.0	0.7568	-6.006	3.456	-8.824
10.0	0.8072	-6.466	3.507	-8.374

TABLE F-6. CURVE FIT COEFFICIENTS FOR θ = 89.9 DEGREES

Energy (MeV)	A	B	C	D
0.5	0.4078	-2.673	1.548	0.2576
1.0	0.3595	-3.365	2.310	-0.03908
2.0	0.3287	-4.155	3.218	-0.4150
3.0	0.3075	-4.997	4.328	-0.9707
4.0	0.2953	-5.465	4.981	-1.321
5.0	0.2846	-6.256	6.104	-1.897
6.0	0.2816	-6.538	6.363	-1.1904
10.0	0.2175	-9.640	11.87	-0.5741

APPENDIX G

EMPIRICAL SCREENING CORRECTION C(E) FOR EQUATION (47) [6]